FINAL TECHNICAL REPORT

External Grant Award No. 04HQGR0080

RUPTURE HISTORY OF THE SAN ANDREAS FAULT AT VAN MATRE RANCH, CARRIZO PLAIN, CALIFORNIA: COLLABORATIVE RESEARCH WITH THE UNIVERSITY OF CALIFORNIA, IRVINE AND ARIZONA STATE UNIVERSITY

Submitted by

Prof. Lisa Grant
Dept. Environmental Health, Science & Policy
University of California
Irvine, CA 92697-7070
949-824-5491 tel 949-824-2056 fax
lgrant@uci.edu

in collaboration with

Prof. J Ramon Arrowsmith
Dept. of Geological Sciences
Arizona State University
Tempe, AZ 85287-1404
ramon.arrowsmith@asu.edu

ABSTRACT

Stream Channel Offset and Late Holocene Slip Rate of the San Andreas Fault at the Van Matre Ranch Site, Carrizo Plain, California

Gabriela R. Noriega[1], J Ramon Arrowsmith[2], Lisa B. Grant[1], Jeri J. Young[2]

[1]University of California, Irvine, Department of Environmental Health,
Science and Policy, Irvine CA 92697-7070
[2]Arizona State University, Department of Geological Sciences, Tempe AZ 85287-1404

Well-preserved channels offset across the San Andreas fault (SAF) at the Van Matre Ranch (VMR) site in the northwestern Elkhorn Hills area of the Carrizo Plain offer the opportunity to measure slip rate and examine geomorphic development of the channels. The fault zone and offset channels were exposed by excavation in one fault-perpendicular and five fault-parallel trenches. The geomorphology and stratigraphy in the channels reveal a record of filling by fluvial sedimentation, lateral colluviation, and pedogenesis**.** The buried thalweg of the currently active channel is offset 24.8 $\pm$ 1 m, while the geomorphic channel is offset approximately 27.6 $\pm$ 1 m. Seventeen samples were collected from channel margin deposits for ^{14}C dating. An OxCal model of the radiocarbon dates with stratigraphic control suggests that the oldest date for channel incision was ~1160 AD. Minimum and maximum slip rates ranging from 29.5 to 35.8 mm/yr result from different assumptions about the timing of channel incision and offset. The slip rates at VMR agree well with the late Holocene slip rate of 33.9 $\pm$ 2.9 mm/yr at Wallace Creek, approximately 18 km to the northwest, and imply that within measurement uncertainty the 30-37 mm/yr velocity gradient across the SAF from decadal time-scale geodetic measurements is accommodated across the several meter-wide SAF zone at VMR over the last millenium.

INTRODUCTION

The southern San Andreas Fault (SAF) south of the creeping section is recognized as southern California's most likely source of future great earthquakes (Figures 1 and 2; WGCEP, 1988 and 1995). The Carrizo Plain (Figures 1 and 2) has been one of the most productive sections of the San Andreas fault for paleoseismic research, yielding late Pleistocene and mid-Holocene slip rates (Sieh and Jahns, 1984), slip per event measurements for the last six ruptures (Liu et al., 2004; Grant and Sieh, 1993; Grant and Donnellan, 1994); and dates of the last five major earthquakes (Grant and Sieh, 1994; Sims 1994). Additionally, from multiple measurements of slip in the most recent 1857 A.D. earthquake (Sieh, 1978; Grant and Sieh, 1993; Grant and Donnellan, 1994), it appears that the San Andreas fault sustained maximum slip in the Carrizo Plain. This section of the fault may control the occurrence of great earthquakes along the southern San Andreas (Sieh and Jahns, 1984; Wells and Coppersmith, 1984) through repetition of similar large events with relatively long recurrence intervals, although some paleoseismic data suggest variable rupture magnitudes and irregular recurrence intervals (Grant and Sieh, 1994; Grant, 1996). These interpretations have different implications for seismic hazard assessment and fault models.

Slip rate is an essential input parameter for either time-dependent or static calculations of seismic hazard on the SAF. Argus and Gordon (2001) determined that 39 $\pm$ 2 mm/yr of relative motion between the Pacific and North American plates is accommodated along the SAF and central California Coast Ranges. The difference between the SAF slip rate and this regional slip budget will indicate the degree of localization of that deformation and the potential for other active seismogenic structures in the Coast Ranges. Sieh and Jahns (1984) reported a slip rate of 33.9 $\pm$ 2.9 mm/yr for the San Andreas fault in the Carrizo Plain over the last 3,700 years, in

agreement with their late Pleistocene rate of ~ 36 mm/yr. Our study provides a latest Holocene slip rate for comparison with late Pleistocene, mid-Holocene and geodetic measurements of deformation. The slip rate is derived from the measurement and dating of offset stream channels. It also provides an opportunity to characterize offset stream channels, and thus improve understanding of their tectonic and geomorphic development.

SITE LOCATION AND HISTORY

The Carrizo Plain is an arid to semi-arid closed basin situated at an elevation of about 580 m. It is physiographically separate from the San Joaquin basin to the northeast and the Cuyama Valley to the southwest by the intervening Temblor and Caliente Ranges respectively (Figures 1 and 2). The Van Matre Ranch (VMR) Site is in the southern Carrizo Plain (Figure 1), approximately 18 km southeast of the multiple paleoseismic sites at Wallace Creek (Sieh and Jahns, 1984; Liu 2003; Liu et al., 2004), Phelan Creeks (Sims, 1994), Phelan fan (Grant and Sieh, 1993) and Bidart fan (Grant and Sieh, 1994). The geomorphic manifestation of repeated ground rupture is evident in the well preserved series of beheaded and abandoned stream channels at VMR (Figures 3-5). Prior to this study Prentice and Sieh (1989) and Sims et al. (1993) conducted reconnaissance investigations of VMR geomorphology and stratigraphy.

This study focuses on offset channel “gully #44,” as reported by Sieh (1977, 1978, 1979; Figures 3 and 5) and investigated by Sims et al. (1993). Sieh documented sites along the SAF where slip from the 1857 A.D. earthquake was well preserved, including VMR. He measured several offset channels numbered 44-50 and postulated that they were formed by 8 ± ½ m displacement in 1857, and two prior earthquakes with 7½ ± 1 m and 10 ± 1 m slip (Figure 3; Sieh, 1978 and 1979).

METHODOLOGY

Trenches were located and excavated based on data from Sims et al. (1993) and Prentice and Sieh (1989). Trenches T2 and T3 (Figure 5) were re-excavations of older trenches. An attempt to re-excavate trench 6 of Sims et al. (1993) was unsuccessful. The resulting trench, T6', is close to T6. Three new trenches (T7, T8, and T9) were also excavated. Trenches excavated in 2004 are labeled T2, T3, T6', T7, T8 and T9 and mapped along with the SAF (Figure 5). T2 was excavated on the northeast side of the fault and upstream of the offset channel. T3 is a fault-perpendicular trench excavated for accurate fault location and investigation of surface rupturing events. T6', T7, T8 and T9 were all excavated on the southwest side of the fault and provide exposures for offset measurements.

Trenches were excavated with a backhoe and supported by hydraulic shoring. The trenches were logged at a scale of 1:25 and the thalwegs were surveyed for spatial control and precise offset measurement. Exposures of the trench walls were also recorded by mosaic photography.

Over 1400 surveyed points define the topography at the site (see Figure 5). Channels once connected to the main channel (southeast) have been offset to the three beheaded channels to the northwest. Our excavations exposed offset channels in trenches T2, T3, T8, T6', and T7. The T7 channel has subsequently captured the small drainage immediately above it. Topographic survey data collected during this project were used to tie all the trenches into the same coordinate system. We also combined new data with pre-existing data (Sims et al. 1993) to produce the topographic map shown in Figure 5 and used them in our offset calculations (see below). In addition, we surveyed all major contacts exposed in the trench walls. Survey data were adjusted from the local datum to an absolute UTM grid projection and the elevation fixed

relative to sea level. Absolute location and elevation accuracy are only several meters (handheld GPS), but the internal precision of the survey is at the cm-level.

In all of the trenches, the stratigraphic units were analyzed, identified, and logged. Sediment and soil analyses were based on unit color, rounding, sorting, clast size, matrix composition, and degree of bioturbation. Sediment analysis and interpretation was the basis for unit correlation and consequently for offset calculation. In each trench, units are numbered in hundreds corresponding to the trench number (e.g. 200 for trench T2). In trenches T2, T3, T6' and T8, correlative units have comparable numbers such that unit 660 in T6' correlates with unit 860 in T8 etc. Numbers increase from oldest (e.g. unit 300) to youngest (e.g. unit 395) within a given trench. Correlations between trenches on the same side of the fault (i.e. T6' and T8) are for the same unit. Correlations of channel units across the fault zone represent the same stratigraphic position.

Radiocarbon analysis and sample pre-treatment for this project was conducted at UCI's Keck carbon isotope AMS facility under the supervision of J. Southon. Standards Ox-I, Ox-II, ANV, and coal 50 thousand years old were used to correct for natural graphitization and AMS fractionation. The dates extracted from the samples were calibrated using atmospheric data from Reimer et al (2004) and OxCal v3.10 Bronk Ramsey (2005). Results are displayed in Table 1 and Supplemental Table 1.

RESULTS

The stratigraphy and abundance of datable materials were favorable for measuring a late Holocene slip rate from the channels exposed in trenches T2, T3, T6' and T8. We exposed the correlative channel in T7, but were unable to date it. T9 exposed deformed old alluvial sediments overlain by young discontinuous channel units that were not definitively correlative

with the offset channels exposed in the other trenches. The following section describes stratigraphy and results of unit correlations between trenches. All stratigraphic units are described in Supplemental Tables 2-7. Trench logs are displayed in Figure 6. Additional trench logs are included in Supplemental Figure 1.

T2-Upstream channel

T2 is a re-excavation of a trench from Sims et al. (1993). The trench is about 7 m long and 3 m wide and exposes relatively young channel deposits on the upstream side of the fault (Figures 5 and 6a). The exposure geometry only preserved short portions of the outer edge equivalents of the southwest wall. Unit 200 is interpreted as local bedrock, mapped as Paso Robles Formation (QTP) on regional maps by Dibblee (1973). Along its upper contact, unit 200 shows downslope warping of units which probably results from soil creep. Unit 200 was incised and then filled to an unknown level by channel deposits and colluvium of unit 210, both of which are bioturbated and subject to bioturbation and accumulation of pedogenic clay, carbonate, and gypsum. Unit 220 fills a channel cut into unit 200/210 with likely coeval colluvial packages of units 240 and 230. (Both units 240 and 230 are burrowed and pedogenically altered, but less so than unit 210). Unit 250 fills a channel cut into units 240/220/230 with roughly coeval colluviation of unit 260 (and lower unit 270). Unit 260 contains numerous clasts from regional unit QTP, presumably derived from some local “bedrock” exposure upslope. Unit 270 at its base is probably the same as unit 260, but then overlies all other units and is in contact with the active soil horizon (Supplemental Table 2) (Figure 6a).

T3-Cross-fault trench

T3 is a re-excavation of a portion of a trench from Sims, et al. (1993) (Supplemental Table 3 and Figure 6b). This is the only trench excavated across the SAF in 2004. Trench T3 clearly shows juxtaposed stratigraphy with unit 300 correlative with the local bedrock unit 200

from trench 2. Unit 300 is a well-lithified grayish unit with silts and thin sands alternating with clast-supported pebbles dominated by Tertiary Monterey formation derived siltstone "chips." Bedding dips to the northeast and the unit is progressively sheared to the southwest until it is completely cut out. At the base of the trench, unit 300 is juxtaposed against 310 across a zone of inferred fissure fill (unit 380). Unit 310 is a tan-beige heterogeneous unit we divided into 3 subunits. Unit 310A is heavily sheared pebbly silt with no clear sedimentary fabric preserved. It grades laterally into unit 310B which is an interbedded sand and silt. Units 310B and 310C are separated by a shear zone unconformably overlain (probably erosionally) by fluvial sand: unit 320. Unit 310C has preserved vertical layering in silt, but it is largely sheared and bioturbated so that the original sedimentary fabric has been obliterated. Unit 310 has some $CaCO_3$ staining further indicating its older age relative to overlying units. Units 330, 340, and 360 represent progressively younger bioturbated and pedogenically modified units. They are silty pebbly sands that do not show any sedimentary structures. Units 350 and 370 on the northeast side of the main fault zone and 375 on the southwest represent the sedimentary fill sequences of the offset channel system that is the primary focus of this study. They are predominantly matrix supported pebble gravels occasionally in upward fining sequences and plain and cross-laminated sands. Unit 395 is the youngest, unfaulted colluvial and fluvial unit.

T3 exposes 3 main shear zones which we interpret as evidence for a minimum of 3 displacement events. The oldest shear zone cuts through unit 300. The southwestern shear zone cuts unit 310 and is unconformably overlain by unit 320. Unit 330 may be cut by a strand of this zone. The most recently active shear zone is capped only by unit 395 and spectacularly disrupts units 375 and 370. Not only are the units sheared, but also one or two distinctly aged fissures are filled in this zone. We infer that the youngest fissure fill formed in the 1857 earthquake.

T6'-first downstream channel

T6' exposed offset channel deposits downstream of the fault (Supplemental table 4; Figures 6c and supplemental figure 1a). The local bedrock is a heavily bioturbated and pedogenically altered tan-beige set of units (610, 620, 630) with occasional (unit 620) to no preserved sedimentary fabric (units 610 & 630). Gravelly unit 640 is the first fill unit into the offset channel. Its basal contact forms one of the thalwegs used to measure channel offset (Figure 5). Unit 640 is overlain by colluvial and/or pedogenically altered units 650 and 660 which are in turn cut by the channel that was subsequently filled by the coarse, angular, crudely bedded gravels in unit 670. In places, the texture of units 630 and 660 are indistinguishable but the contact between them is well defined by a color contrast with darker unit 660 above lighter units 630 and 610. Several ^{14}C samples were collected in trench T6'. However, only sample T6'-4 from the top of unit 630 yielded a reliable date which gives a maximum channel age (See radiocarbon dating section).

T8-first downstream channel

Coarse, angular, stratified gravels in units 840 and 870 with scour and fill structures are interpreted as channel fill deposits in trench T8 (Supplemental Table5; Figures 6d and supplemental Figure 1b). The base of 840 is the offset thalweg we matched with that exposed in T6' and T2.The channels were cut into units 810, 820 and 830, which are interpreted as colluvium. Unit 860 is a clayey silt deposit containing most of the radiocarbon-dated samples near its top. It could be either colluvium, washed down from adjacent hill slopes, or autochthonous alteration of channel deposits by bioturbation and other pedogenic processes. Most of the samples collected for dating were retrieved from this trench.

T7-second downstream channel

Because of its older age, the stratigraphic relationships in trench 7 (Supplemental Table 6; Figures 6e and supplemental 1c) are more obscured by pedogenesis than in the younger trenches. Nonetheless, unit 730 has eroded into the local bedrock (a Quaternary fan deposit) and its base represents the thalweg that we correlate with that exposed in Trenches 2, 6' and 8. This channel thalweg is offset about 48.8 m. Unit 740 is heavily pedogenically altered, but preserves a few channel gravel packages. Colluvial unit 750 dominates the upper portion of the exposure. Unit 760 has occasional disseminated lenses of coarse, angular to subangular sand and very fine angular pebble gravel within a more massive clayey, sandy silt. This unit most likely represents erosion and fill from the smaller watershed that the T7 channel has recently captured (Figure 5).

RADIOCARBON DATING

Carbonaceous samples collected from the excavations were large enough for radiocarbon dating and sufficiently numerous to provide age control for the units from which they were collected. Most of the samples dated were located in trenches T6' and T8. Results of radiocarbon dating of samples most relevant to determination of slip rate are presented in Table 1.

Results for all samples are in Supplemental Table 1. Potential complications with age control in the Carrizo Plain include inherited age from detrital wood, the presence of shrubs that can live more than 800 years (Grant and Sieh, 1993) and anomalously old radiocarbon ages of terrestrial gastropods (Grant and Sieh, 1994). Three anomalously older dates were obtained from gastropod shells collected in trench T8 and from an undisturbed surface sample from outside the trenches.

The most relevant samples were collected from channel margin clayey silts (units 860 and 630) and channel fill deposits (unit 870) bounding the lower part of the channel margin in trenches T8 and T6'. None of the dated samples was indisputably collected from within the

channel fill. Samples T8_8 and T8_11 were collected along a diffuse contact between channel fill (unit 870) and channel margin (unit 860). The older sample, T8_8, (Supplemental Table 1) has a median probability date up to two centuries older than other samples from unit 860 and therefore is presumed to be reworked.

The date of channel cutting or maximum age of channel offset is obtained from analysis of the dates and stratigraphic positions of samples (shown in Table 1) and output from the program OxCal v. 3.10 (Bronk Ramsay, 1995, 2001). The stratigraphically lowest samples are T6'-3 (Supplemental Table 1) and T6'-4 (Table 1). Sample T6'-3 is a millennium older than other samples, is presumed to be reworked, and therefore is not included in the analysis. Sample T8-11 was collected from the outermost channel fill, or the channel margin. The remaining samples in Table 1 were collected from within unit 860. An OxCal model (Supplemental Figure 2) was constructed to sum the cluster of seven samples from T8 and place samples T8-11 and T6'-4 in stratigraphic order. The results constrain the maximum age date of channel incision (1165 AD) to approximately the minimum age of sample T6'-4 (1165 A.D., see Table 1).

TECTONIC GEOMORPHOLOGY

The VMR site preserves a spectacular set of offset channels (Figures 3-5). They drew the attention of Sieh (1977, 1978, and 1979) who emphasized the study of channels 47-48 because they preserved the record of the last offset (8 ± 0.5 m). Channels 48, 46, and 45 were offset such that the penultimate offset of 7.5 ± 1 m could be estimated. Channel 44 is offset 27 ± 2.7 m according to Sieh, (1977) and in combination with the other offsets at the site, yields an offset in the 3rd event back of about 10 ± 1 m. The offset history is interpretable because of the excellent preservation of the channels and because of the clear record of incision, offset and abandonment (Figure 3). However, the number of slip events that generated each offset cannot be determined

directly from the geomorphology. Evidence from trench T3 indicates a minimum of 3 slip events contributed to the offset of Sieh's channel 44 (our study site). As described in the discussion, evidence from other studies suggests a maximum of 5 or 6 slip events.

The pattern of geomorphology and stratigraphy at VMR implied the following model by Sims et al (1993; see also Sims, 1994) of tectonic offset and subsequent channel response: 1) A new channel is cut or inherited. 2) After initial offset, the channel may continue to incise. 3) Continued offset and channel lengthening decreases local along-fault channel gradient, causing sedimentation as shingled, nested cut-in-fill channel deposits. 4) Further offset along the fault promotes increased deposition and filling of the channel. The filled channel may be capped by fan deposits and allow incision of a new channel across the fault or be captured by a topographic low juxtaposed by recurrent offset. Channel 44 is in this latter stage in its current configuration. There is little "room" in the channel for further deposition and it is likely to be abandoned soon (and will probably occupy a channel initially formed by channel 45; Figures 3-5).

The geomorphology and stratigraphy in the channels reveal a record of filling by fluvial sedimentation, lateral colluviation, and pedogenesis. Typically, the channel units (e.g., 220, 250, 640, 670, 840, 870, 730, and 740) cut into or are overlain by reworked fluvial units (210, 230, 240, 260, 270, 650, 660, 680, 860, 880, 700-720, and 750). The older reworked fluvial units usually contain $CaCO_3$ that gives them a light color. In places, the basal boundary for the older colluvial units is diffuse (portions of T2) or sharp and scalloped (T9).

We have developed two end-member models for the development of the reworked fluvial units. In the first model the heavily bioturbated and pedogenically altered fluvial sediment no longer has sedimentary fabric preserved. This model is supported best by the relationships from T2 in which units 230 and 240 grade into the central channel unit 220 (Figure 6a). In the second

model colluvium is delivered to the channels during the relatively long periods of no fluvial transport in the channels. The colluvium shows interfingering relationships with the channel sediments. For example, T8 (Figure 6d) has a wedge of colluvial material (unit 860) overlying the channel fill (unit 840), and is cut by unit 870.

The possibility of gullies, to the southeast of our study site, sourcing channels that would align with our gully is rejected by geomorphic and stratigraphic evidence. Strike-slip motion could have not have caused channelhead #44 to line up with the older tails of channel #45 of our study and create an apparent offset. The displacement necessary to place the channel at this site location would be greater than the current acceptable displacement given the ages of the dated samples.

OFFSET MEASUREMENTS

To measure the channel offsets, we surveyed the geomorphic trace of the San Andreas fault at VMR (N56W) and projected the trench survey data that define the offset channel buried thalwegs to either be parallel or perpendicular to the trace. The projection is also approximately parallel or perpendicular to the orientation of the trench walls. The distance along the fault versus elevation of the surveyed buried channel thalweg for the two walls of each trench (and topographic profile along the SAF through the trenches) is shown in the lower plot in Figure 5. The offset is measured as the relative distance between the lowest point in the T2 NE channel thalweg and the thalweg centers. We measured it for the pairs of buried offset channels in T2-T6', T2-T8, T2-T7, and the associated geomorphic offsets from the surveyed topography. We did not make such a determination for T9 because evidence for an identifiable buried channel thalweg was ambiguous (see Supplemental Figure 1d).

Results of offset measurements from surveying are displayed in Table 2. The buried thalweg of the currently active channel is offset 24.8 m, with a qualitatively defined conservative measurement uncertainty of +/- 1 m. The geomorphic offset is 27.6 m. The geomorphic offset has significantly higher uncertainty because the geomorphic thalweg is broader and not as well defined as the buried thalweg.

The thalweg of the first beheaded channel that is exposed in T7 is offset 48.8 m with a geomorphic offset of 51.8 m. The geomorphic offset of the second beheaded channel that we tried to expose in T9 ranges from 71.9 to 79.0 m. There were no datable materials in trenches T7 and T9. As a result, only the downstream channel exposed by T6' and T8 is used for slip-rate measurement.

SLIP RATE

Slip rate is obtained from channel offset divided by time interval. The accuracy and precision of the slip rate depends on how accurately and precisely the measured parameters represent the actual tectonic offset of the channel. We measured offset of the buried thalweg, as exposed in the walls of trenches (24.8 m $\pm$ 1m), and as expressed by surficial geomorphology (27.6 m $\pm$ 1m). For slip rate measurement, the buried thalweg is a better representation of channel offset because it is better defined morphologically and because it was formed at the time of initial channel incision. As described in the section on radiocarbon dating, the maximum age of sample T6'-4 (approx. 1165 AD) provides a maximum age for incision of the channel, which post-dates deposition of the sample.

A minimum slip rate, 29.5 mm/yr, is derived from offset of the buried thalweg (24.8 m) divided by the maximum time interval (2005 AD – 1165 AD). This scenario assumes that the

channel was offset immediately following incision and uses the maximum possible date of incision as defined by sample T6'-4 and results of the OxCal model.

It is likely that some time passed between channel incision and offset. A faster slip rate can be derived based on the assumption that the channel was incised circa 1165 AD and offset by surface rupturing "Event E" of Grant and Sieh (1994) dated 1218-1276 AD. A shorter time interval of measurement would be the time since the youngest date of this event (2005 - 1276 AD). The resulting slip rate is 34.0 mm/yr. This slip rate is in excellent agreement with the late Holocene slip rate of 33.9 $\pm$ 2.9 mm/yr measured at Wallace Creek (Sieh and Jahns, 1984).

A maximum slip rate can be derived from a shorter time interval. For example, the date of the most recent slip event, the 1857 AD earthquake, could be used as the end point of the time interval to obtain a slip rate of 35.8 mm/yr (i.e. 24.8 m / [1857 – 1165 AD]). This slip rate also agrees well with Sieh and Jahns (1984) late Pleistocene measurement of ~36 mm/yr at Wallace Creek.

DISCUSSION

This study fills a temporal gap between current deformation rates (Argus and Gordon, 2001; Titus et al., 2005; Lisowski et al., 1991) and older slip rates reported by Sieh and Jahns (1984). The minimum late Holocene slip rate at VMR is 29.5 mm/yr and the maximum rate is 35.8 mm/yr, in excellent agreement with older rates reported at Wallace Creek. This result suggests that the slip rate has not changed measurably over the last few centuries to few millennia. The slip rate at VMR also provides insight into slip partitioning between the San Andreas fault in the Carrizo Plain and deformation in the Coast Ranges, as well as the degree of localization of faulting.

Figure 2 shows the SCEC Crustal Motion Model 3 (Shen, et al., 2003; http://epicenter.usc.edu/cmm3/) from which we selected those velocities in a ~100 km wide swath perpendicular to the SAF centered on the Carrizo Plain. We projected them to the N40W direction to determine a velocity parallel to the average trace of the SAF northwest of the Transverse Ranges (note that projecting them to N56W—local VMR SAF trace--only changes the gradient by 1-2 mm/yr). The N40W velocity profile shows a steep gradient of about 30 mm/yr across the SAF at the Carrizo Plain. Assuming that these data represent steady interseismic motion, these data can be interpreted by calculating the surface displacement profile from strike-slip from the brittle-ductile transition zone (here assumed to be 12 km) to great depth (e.g., along an infinitely long vertical screw dislocation; Thatcher, 1990). Two curves for 30 and 37 mm/yr of steady deep slip approximately bound the observed velocities in figure 2. Further detailed analysis of these data is beyond the scope of this paper, but clearly they are consistent with the slip rate we have determined. Importantly, the slip at the VMR site indicates that all of the regional shear of the SAF system in the area of the Carrizo Plain likely has been accommodated across a narrow, few-meter wide fault zone for the last millennium.

If the deformation is so localized at the VMR site, an interesting question is how many surface ruptures generated the measured offset. Sieh (1978) proposed that the last 3 ruptures at VMR involved 8, 7 ½ and 10 m slip respectively, for a total offset of 25 ½ m. Detailed logging of trench T3 revealed evidence of at least 3 ruptures, but the total number of events could not be discriminated due to laterally discontinuous cut-and-fill channel stratigraphy. From extrapolation of findings at Wallace Creek (Liu et al., 2004), the number of earthquakes could range from three to six. At Wallace Creek, displacement from the last 5 ruptures totaled 22.1 m. Therefore,

at VMR the 24.8 ± 1 m offset of the buried thalweg could have been produced by 5 or 6

comparable ruptures, with an average dextral slip of 4 to 5 m each.

ACKNOWLEDGEMENTS
We would like to thank John Sims and John Hamilton of USGS for sharing the 1993 data and working with Arrowsmith to develop the site. We would also like to thank Mr. Leonard Bidart for granting us permission to work on Bidart Brothers property. Comments of J. Lienkaemper and an anonymous reviewer contributed substantially toward improving the manuscript. We are especially grateful for Lienkaemper's expert and specific advice about constructing an appropriate OxCal model. Thanks to the Keck Carbon Cycle AMS lab staff at UCI, and especially Drs. John Southon, Guaciara M. Dos Santos and Susana E. Gonzalez for training and supervision. Nathan Toké, Kenneth Jones, Raymond Ludwig and Frank Romaglia are thanked for help in the field, and Olaf Zielke for digitizing. Miryha Gould and Eric Runnerstrom produced images shown in figure 3 from aerial photography and elevation data provided by Kerry Sieh. Thanks to Hector Hernandez for constant help, support and constructive criticism. This project was supported by the United States Geological Survey (USGS), Department of Interior, under USGS award 04HQGR0080, and by NSF EAR 0409500 and EAR0409745 to Grant and Arrowsmith. Shoring was provided by the Southern California Earthquake Center. SCEC is funded by NSF Cooperative Agreement EAR-0106924 and USGS Cooperative Agreement 02HQAG0008. The SCEC contribution number for this paper is 906.

TABLES

Table 1. ^{14}C data for slip rate determination for the VMR paleoseismic site. See Supplemental Table 1 for all ^{14}C determinations. All analyses are standard AMS dates from the UCI Keck Carbon Isotope facility. Calibrated dates are from OxCal Program v3.10 (2005).[1,2]

Sample code	Description	Radiocarbon Age BP	+/-	$\delta^{13}C$	σ	cal A.D. age Ranges	Stratigraphic Unit
T8_10	wood	675	20	-7.5	1	1280-1380	860
					2	1270-1390	
T8_5	charcoal	675	20	-19.0	1	1280-1380	860
					2	1270-1390	
T8_4	charcoal	630	20	-18.5	1	1295-1390	860
					2	1280-1400	
T8_1	charcoal	615	25	-16.8	1	1300-1395	860
					2	1290-1400	
T8_3	charcoal	705	20	-9.7	1	1275-1290	860
					2	1260-1380	
T8_2	charcoal	630	25	-22.2	1	1295-1390	860
					2	1280-1400	
T8_9	charcoal	665	20	-11.4	1	1285-1385	860
					2	1270-1390	
Summed Dates Probability					1	1270-1390	860
					2	1270-1400	
T8_11	charcoal	795	20	-14.6	1	1220-1260	870
					2	1215-1270	
T6_4	wood	830	20	-18.9	1	1185-1255	630
					2	1165-1260	

[1]Radiocarbon concentrations were given as fractions of the Modern standard, D14C, conventional radiocarbon age and DEL14C, following the conventions of Stuiver and Polach (Radiocarbon, v. 19, p.355, 1977). See supplemental Table 1.

[2]AMS - d13C values were measured on prepared graphite using the AMS spectrometer. These can differ slightly (typically by 1-3‰) from those of the original material, if fractionation occurred during sample graphitization

Table 2. Offset calculations. The lowest surveyed point from T_6' and T_8 was used to measure offset from lowest point of T_2. See Figure 5.

Wall	**Offset (m)**
T8NE	25.0
T8SW	25.5
T6primeNE	24.4
T6primeSW	24.4
Average	**24.8**
Geomorphic offset	27.6

Supplemental Table 1. Radiocarbon Data

KECK CARBON CYCLE AMS FACILITY

EARTH SYSTEM SCIENCE DEPT, UC IRVINE

UCIAMS #	Sample name	Other ID	AMS - del13C (‰)	±	fraction Modern	±	D14C (‰)	±	14C age (BP)	±	DEL 14C	±
9309	UCIG3672	T6'_3*	-8.5	0.7	1.0453	0.0057	45.3	5.7	-350	45	38.5	5.7
9310	UCIG3673	T6'_4	-18.9	0.1	0.9018	0.0021	-98.2	2.1	830	20	-104.1	2.1
9311	UCIG3676	T7_4*	-6.0	0.3	0.7938	0.0016	-206.2	1.6	1855	20	-211.4	1.6
9314	UCIG3677	T7_5 snail*	-10.9	0.3	0.9243	0.0019	-75.7	1.9	635	20	-81.7	1.9
9315	UCIG3680	T8_3	-9.7	0.1	0.9158	0.0019	-84.2	1.9	705	20	-90.1	1.9
9316	UCIG3681	T8_4	-18.5	0.3	0.9246	0.0019	-75.4	1.9	630	20	-81.4	1.9
9319	UCIG3682	T8_5	-19.0	0.3	0.9192	0.0018	-80.8	1.8	675	20	-86.8	1.8
9320	UCIG3683	T8_6 snail*	-1.8	0.3	0.8227	0.0016	-177.3	1.6	1570	20	-182.6	1.6
9321	UCIG3684	T8_7 snail*	-1.8	0.2	0.9294	0.0023	-70.6	2.3	590	25	-76.6	2.3
9322	UCIG3685	T8_8*	-18.5	0.2	0.8937	0.0018	-106.3	1.8	905	20	-112.1	1.8
9325	UCIG3686	T8_9	-11.4	0.2	0.9204	0.0018	-79.6	1.8	665	20	-85.6	1.8
9326	UCIG3687	T8_10	-7.5	0.2	0.9193	0.0018	-80.7	1.8	675	20	-86.7	1.8
9327	UCIG3688	T8_11	-14.6	0.2	0.9057	0.0022	-94.3	2.2	795	20	-100.2	2.2
9329	UCIG3712	vmr_uss modern snail*	-5.3	0.2	0.9339	0.0020	-66.1	2.0	550	20	-72.2	2.0
9330	UCIG3738	T8_1	-16.8	0.2	0.9260	0.0023	-74.0	2.3	615	25	-80.0	2.3
9331	UCIG3739	T8_2	-22.2	0.7	0.9245	0.0024	-75.5	2.4	630	25	-81.5	2.4
9596	UCIG3778	SR5156 whale bone	-14.7	0.1	0.0034	0.0002	-996.6	0.2	45730	400	-996.7	0.2
9599	UCIG3669	T2_1(B)**	-24.3	0.4	1.1421	0.0036	142.1	3.6	-1065	30	134.7	3.6

Radiocarbon concentrations are given as fractions of the Modern standard, D14C, conventional radiocarbon age and DEL14C, following the conventions of Stuiver and Polach (Radiocarbon, v. 19, p.355, 1977).

Sample preparation backgrounds have been subtracted, based on measurements of 14C-free coal (organics), calcite (carbonate) and Whale bone (bone - UCIG# 3778).

AMS - d13C values were measured on prepared graphite using the AMS spectrometer. These can differ slightly (typically by 1-3‰) from those of the original material, if fractionation ocurred during sample graphitization.

*Excluded dates. USS: undisturbed surface snail

**Bone sample. Excluded.

Supplemental Table 2. Stratigraphic unit descriptions for Trench T2.

200 QTP	5Y 7/3 Light gray pale yellow. Paso Robles Fm. Medium coarse, well indurated, clayey, fine, sandy silt. Sub-angular to sub-rounded sand and pebbles lenses, coarsening upward overall. Bedding parallel faults along silt-clay bedding planes. Coarsening upward into poorly to well sorted fine-medium sands. Also contains angular pebble stringers (poorly sorted) –coarse sand to medium pebbles (average is fine pebble). Medium bedded (5-20 cm) sands and gravels with massive units (>20cm). Some fining upward packages. Crude fine bedding in some sands and gravels. Some gypsum accumulations near upper contact. $CaCO_3$ cemented.
210	5Y 7/2 Light gray Mudstone, fine sandstone and matrix supported pebbles. Approximately 15 cm thick with approximately 3 cm gradation to upper unit. Disappears towards bottom. Lower in mobile upper portion of QTP (Dibblee, 1973). Alternative contact for QTP at top of it. Thinly bedded, inclined toward paleochannel. Derived locally from QTP below and upslope.
	Upper 5Y 7-6/4 Pale yellow-Pale olive Massive clayey silty pebbly sand. Very friable. Gypsum and $CaCO_3$ filaments and cement. Occasional pebble and sand lenses- possibly relict bedding (4-5 cm thick, 12-14 cm long). Contains occasional clasts of QTP. Sharp contact at base in lower portion with QTP.
220	5Y 7-6/4 Pale yellow- pale olive Angular pebble-gravels towards base with cut in fill structures. Grades upward into coarse to fine sand. Poorly sorted. Some discontinuous silty laminae are present. Not as well organized as 250 (likely bioturbation). Grades laterally into 230 and 240. Clasts are granite (dominates), metasediments, feldspar, coarse gray sandstone, hard mudstone, quartz, mafic crystalline rocks.
230	5Y 7/3 Pale yellow Fine sandy silt, with clay and pebbles. Lateral gradation to SE from 220. Massive, structure less, likely bioturbated. Some gypsum with $CaCO_3$ filaments disseminated
240	5Y 7/3 Pale yellow Fine sandy silt, with clay and pebbles. Lateral gradation to NW from 220. Structureless, likely bioturbated. Base is olive sandy silt grading upwards from QTP.
250	5 Y 7/3 Pale yellow Sub-angular to sub-rounded poorly sorted grains; quartz, feldspar, mafics, granite pebbles, meta sediments. Laminated silts: some planar, some dipping or trough shaped. Coarse angular sand lenses. Fine to medium sand lenses. Shallow scour-in-fill structures (3 cm high). Basal coarse pebble sand with coarse materials in the center. Few small lenses of fine-pebble sub angular clast supported. Occasional angular cobbles towards top, but overall unit is less bedded upwards, and shows more colluvial input upwards
260	5Y 6/3 Pale olive Medium-coarse pebbly sandy silt. Pockets of predominantly QTP-derived clasts approximately 5-10 cm in diameter. Structureless debris flow or slope wash. No filaments. Does react with HCl. Includes some gypsum blebs.
270	5 Y 7/3 Pale yellow Very fine, densely bioturbated, structureless, clayey sandy silt. Rooted, slightly more organic towards the top. At base has some pebbles. Fewer random clasts than 260.

Supplemental Table 3. Stratigraphic unit descriptions for Trench T3.

300 QTP	5Y 7/3 Light grey pale yellow Pebbly sandy clayey silt. Interbedded, well-sorted fine-medium sand with massive pebbly sandy silts and silts. Highly fractured in SW half of its exposure. Strongly cemented by gypsum in fractured zone. Somewhat less indurated near the top. Contains filament sand nodules in upper portion. Pebbles are clustered in places. Rock types include granite, dark mafic crystalline rocks, Monterey Formationderived laminated mudstone (Dibblee, 1973), and quartz.
310	A) 2.5Y 7/4 Pale yellow Cobble-pebble sandy silt. Well indurated, massive. Fractured along NE side. Clasts are predominantly crytaline and the granotoids are deeply weathered to grus. Subangular to subrounded small cobbles. Well cemented by gypsum and $CaCO_3$. Some steeply dipping tectonic fabric.
	B) 2.5Y 7/3 Pale yellow Interbedded highly fractured well-indurated fine sand, silt and subangular to subrounded pebbly coarse sand. Beds are approximately 10 to 20 cm thick. Silt and mudstone are finely laminated to massive. Pebbly zones are mostly clast-supported. Upper portions is less indurated and may have been weathered. May grade into 310 below. Appears to mostly be a coherent block.
	C) 2.5Y 7/3 Pale yellow Massive on bedded well indurated silt and fine sand. Bedding is a few cm think. One zone of pebbles is evident on 1993 log. Top appears to have been sculpted and then buried by 320. Pervasively sheared in most places.
320	Sandy silt well bedded with gravel lenses incised into it. $CaCO_3$ nodules along the top.
330	2.5Y 7/3 Pale Yellow Clayey very fine sand silt. Mostly massive and densely bioturbated. Coarse sand to pebble sized clasts distributed throughout. Few $CaCO_3$/gypsum blebs (white). Sheared at base. Numerous $CaCO_3$/gypsum filaments in upper portion. Contains numerous QTP clasts. Some are dismembered and soft (weathered) while others are still well indurated. South-west of trench color change 2.5Y 5/2 light olive brown
340	2.5Y 6/4 Light yellow brown Similar to 330, darker in color. Fewer $CaCO_3$/gypsum blebs/filaments. Small sandy pieces possibly from burrows. Higher percent of coarse sand and pebbles than 330, but may grade into 340.
350	2.5Y 6/4-3 Light yellowish brown Relict and real bedding in places, massive in others. Upper contact is gradational with 370. Angular poorly sorted very coarse to fine sand lenses and stringers interbedded with laminated and crossbedded silt and very fine angular pebble gravel.
360	Massive clayey-pebbly sandy silt. Chaotic distribution of clasts. Well bioturbated. Gradational boundary with 330
370	2.5Y 6/4 Light yellowish brown Big scour with angular very coarse sand with fine to large pebbles clasts. Very fine sand and coarse silt, 3 to 5 cm interbeds with gravel lenses and stringers (coarse sand to fine pebble with occasional small pebble clasts). Mostly subangular with occasional subrounded clasts. Patchy uncommon $CaCO_3$ coating and blebs (white) and filaments. Poorly sorted overall. Bimodal sand/silt and gravels. Fine scour and fill structures. Clasts: granite, meta sediments, quartz, feldspar, and gypsum crystals.

375	2.5Y 6/3 Similar to 370. Not as clearly preserved sedimentary structures. Notable laminated very fine sands to very fine silts about 2.5 cm thick with multiple laminae. Disseminated laminated coarse silts. Shallow scour of gravel grading laterally into a gravel stringer. Scour of gravel (lens) subangular to subrounded coarse sand to medium pebble, average is fine pebble. Other shallow scours grading from coarse to fine sand. The rest is mostly structureless with exception of occasional fine silt. Clast: granites, feldspar, quartz, and metasediments. Basal contact is gradational with adjacent/underlying colluvium.
380	2.5Y 6/3-4 Light yellow brown Pebbly-clayey sandy silt with cobble aligned with fault zone. Clasts include mafic fractured granotoid and quartz clasts. Some sand packages appear sheared. Three main bodies with sand in zones on outside and the large clasts in the middle. Likely fault gouge.
390	2.5Y 6/3-4 Light yellow brown Better presentation of sedimentary structures in blocks of 370/375 with pockets of subrounded clasts supported gravel: fine sand to medium pebble. Upper part is poorly sorted medium sand to fine pebble. Upper portion comprised of blocks tilted and probably fallen into an open fissure. Same zones are pebbly sands with disseminated silt breccia. Notable silt from 375 is clear marker of deformation. Top has approximately 20 cm paleorelief as it was buried by 395.
395	Modern O horizon. Buried -very thin- organic layers between the major units. Predominantly massive pebbly sand. Meter-scale tabular units.

Supplemental Table 4. Stratigraphic unit descriptions for Trench T6'.

610	Older fan and colluvial gravel fan unit has compact bladed sedimentary soil structure in northern end of trench on SW wall and is difficult to visually distinguish from unit 620. More indurated than unit 620. On NW wall it dips steeply beneath a well-defined contact with unit 620.
620	Older fan unit appears to be dipping to the east. It is more indurated than the channel sediments; range of clast sizes is coarser than the channel sediments. Distinct beds of gravel and beds of sand exposed on northern wall; angular; greater that ¼ of the clasts are covered with rinds of caliche. Clast types: large cobbles of marble and basalt,, pebbles of granite and angular greywacke clasts
630	Pale yellow older colluvium with gravel. Similar to unit 830. Well defined contact between unit 630 and overlying unit 660. Contact is $CaCO_3$ rich, with unit 630 defined by lighter color..
640	Very coarse to coarse grained, poorly sorted channel gravel. No caliche rinds. Similar to unit 840.
650	Colluvial or silty soil unit containing coarse crystalline angular granite boulder on SW wall. Darker than underlying units, with lower contact well defined by color contrast.
660	Green-tan-light brown silty colluvial or soil unit with gravel. Darker than underlying units. Lower contact well-defined by color contrast. Same cobble of QTP in channel deposit, contains green-gray mudstone.
670	Main channel. Interbedded gravel with fine grained, vary thinly to thinly bedded moderately to well sorted sub rounded (to angular) sand with coarse, sub-angular sand lenses. Gradational contact with 680; disseminated layers above more continuous layers. SE contacts are diffuse.
680	Fine grained, poorly indurated and bioturbated silty sand and sandy silt. Similar to unit 880.

Supplemental Table 5. Stratigraphic unit descriptions for Trench T8.

810	2.5Y 6/4 Pale yellow Very coarse grained, angular to sub-angular, massive, very well indurated, structureless, thin wedge, bedrock? Difference between 810 and 820 is that 810 is more indurated. Contains filaments and “worm” of carbonate or gypsum.
820	2.5Y 7/4 Pale yellow Fine grained to coarse grained, poorly sorted, angular to sub-angular, structureless, moderate to poorly indurated, sandy silt. Overlays a more indurated coarser grained 810 unit. Contains poorly developed caliche rinds.
830	2.5Y 7/3 Pale yellow Very fine grained, poorly sorted, massive, angular to sub-angular, poorly to moderately indurated, matrix supported, silt. With burrows (2x8cm), colluvium underlays 860. Distinctive difference is the lighter color, which marks the boundary.
840	Very coarse to coarse grained, poorly sorted, moderate to well indurated, angular to sub-rounded, massive gravel. Unit is dense. Underlays younger channel 870. Structureless. Clasts up to 10 cm in diameter. Clast supported. Cuts into 810, 820 and 850. Some clasts are up to 18x14 cm.
850	2.5Y 7/4 Pale yellow Similar to 880 has more $CaCO_3$. Contains subvertical fabric in pebbles, mineralized fractures and fine-grained sediments (rip-up clasts).
860	2.5Y 6/4 Very fine grained, poorly sorted (up to 8 mm), angular to sub-angular, poorly indurated, medium laminated (average 9cm x 3cm). Brown silt, with burrows (4x14cm). Matrix supported, non-fossiliferous, extensively rooted, soil.
870 Main channel	2.5Y 6/3 Light yellowish brown Angular to sub-angular, moderate to well sorted, highly laminated, cross-beds, gravel lenses and sand lenses, thin to medium laminations, clasts up to 10cm, scours into 810, 850 and 820, 830 and 860. Gravel lenses range from 15x8 to 40x10 cm, sand lenses average 30x20, 50x10, lenses consist of several scouring channel events. Highly rooted SE side. Samples T8_8, 11, 3, 2, 9, 1 (a, b), 10 were collected in T_8. Contact with 840 sharp. Interfingers with 880, 820, 860
880	2.5Y 7/4 Pale yellow Fine grained, moderately to well sorted, sub-angular to sub-rounded, massive, poorly indurated, medium laminated and heavily bioturbated silt.
890	Massive, well-indurated, angular, poorly sorted gravel.

Supplemental Table 6. Stratigraphic unit descriptions for Trench T7

700 Old Fan QTP	2.5Y 6-7/4 Light yellowish brown. Paso Robles Fm. Alternating, vertical layers of coarse, angular gravel sand with poorly sorted angular median and coarse sand lenses; gravel lenses; and fine silt lenses. Gravel includes very small pebbles to large cobble, average-medium angular to subangular polymictic pebble gravel. Gypsum roses developed on some sands. Some $CaCO_3$ cement, but overall very friable. Gypsum "roses" are developed interstitially and below 710 unit, within 700.
710	2.5Y 7/4 Pale yellow Massive, densely bioturbated, largely angular gravel near base. Partial $CaCO_3$ coating on grains, contains more $CaCO_3$ than surrounding layers or units.
720	2.5Y 6/7 Light yellowish brown Clayey sandy silt, random clasts throughout. Some clasts are up to medium cobble size. Partially $CaCO_3$ coated. Contact grades into 710.
740	2.5 Y 6/4 Light yellowish brown Massive clayey sandy silt with random angular fine pebble clasts. Disseminated sand and fine gravel lenses. ^{14}C samples collected from this unit
750	2.5Y 6/4 Light yellow Massive, clayey sandy fine silt. Contains random fine pebble clasts throughout, contact contrasts with lower 710 unit. Grades into 740 and 760.
760	10Y 6/3 Pale brown Lenses of coarse, angular to subangular sand and very fine angular pebble gravel within more massive clayey, sandy silt. Occasional disseminated sand lenses.
770	2.5Y 5/4 Light olive brown Clayey silty to very fine sand. Occasional random angular fine cobble size clasts.

Supplemental Table 7. Stratigraphic unit descriptions for Trench T9.

910	2.5Y 7/3 Pale yellow Older alluvial fan unit with steeply dipping beds of indurated silt, silty sand and silty sandy gravel. Beds are subparallel to the trench and undulate so that the exposure on the NE wall shows “windows” of different beds and apparent dips. Several “caves” formed in both walls along bedding plane failures. Attitude on a siltstone bed at the SE end of the trench is N35W 70°SW. Exposures of silty sand sandy gravel, and silty sand or sandy gravelly silt. Maximum clasts size is 22 cm. Many clasts have well developed rinds of carbonate or gypsum. Coarse plutonic clasts have grusified. Crystal roses of gypsum and “spaghetti worms” (2-5 mm) of gypsum are scattered, but concentrated in some places. Clasts are mostly well rounded ranging to subrounded or subangular, clasts are dominantly coarse and fine crystalline rocks.
920	2.5Y 7/4 Pale yellow Sandy gravel and silty sandy gravel lenses and small channels with sharp, scoured contacts in a matrix of gravelly silty fine to coarse sand with pebble stringers. Several small channels have fining upward sequence of granule to fine sand. Scattered specks (2-5 mm) of chalky white minerals could be gypsum or calcite. Maximum measured clast size is 12 cm. Dominant clast lithology is igneous (felsic and mafic, primarily plutonic with some volcanic). Foliated metamorphic, and quartz rich clasts also present. Most clasts are well rounded. 20 to 40% are angular. Most clasts do not have mineral coatings or rinds. The upper contact with unit 930 is sharply defined by color change. The upper edges of the channel are gradational with unit 910.
930	2.5Y 6/4 Light yellowish brown Massive silty gravelly sand to silty coarse sand with abundant rootlets, roots and poorly defined suspected infilled burrows. This unit extends to the ground surface. A well-defined scoured channel is filled with stratified coarse sand and pebbles, grading upward to pebbly sandy silt and pebbly sand, near the SE end of the trench, visible on both walls. The upper part of the small channel may be bioturbated and is gradational with the rest of the unit.

FIGURE CAPTIONS

Figure 1. A) Major historic ruptures along the San Andreas Fault (SAF; modified from Allen, 1968) showing location of Van Matre Ranch site (VMR) in northwestern portion of SAF that ruptured in the 1857 earthquake. B) Aerial photograph mosaic of Carrizo Plain showing active fault trace observations from Vedder and Wallace (1970) as well as locations of Bidart Fan (BF), Phelan Fan (PF), Wallace Creek (WC) and Van Matre Ranch (VMR) paleoseismic sites. Polygon at VMR shows the location of aerial photography in Figure 3.

Figure 2. A) Shaded relief, active faults (modified from http://qfaults.cr.usgs.gov/) of Southern California and selected site velocities from the Southern California Earthquake Center Crustal Motion Map (CMM3; Shen, et al., 2003). White triangles show all CMM3 sites in the region, and those we selected from the group have velocities shown by arrows (note the velocity scale at the bottom). The maximum velocity uncertainty is 4.6 mm/yr, but the maximum in the N40W direction is 1.6 mm/yr. The clear velocity gradient across the SAF is shown in B. The location of the VMR site is indicated by the star. B) The N40W parallel component of the selected CMM3 velocities is plotted with respect to distance from the SAF and relative to 0 mm/yr at the SAF. The two curves show modeled velocities for steady interseismic slip below 12 km and bracket most of the observed motion. At left, the slip rate estimate from our study of 29.5 to 35.8 mm/yr with uncertainties indicated by the white boxes is drawn for comparison.

Figure 3. A) Rectified aerial photograph (3-9-1991; original scale 1:3,000) showing the clear traces of the SAF at the VMR site (see Figure 1 for location) with numerous small offsets (those studied by Sieh, 1978 are shown with corresponding numbers). In this study, we focused on channel 44 (the outline of Figure 5 is shown by the black rectangle). B) Oblique view to the east-southeast of aerial photo draped over photogrammetrically-produced and digitized elevation data.

Figure 4. A) Overview to the west of the VMR site. The arrow shows the view direction of B. B) View southeast along the SAF showing the upstream channel segment at the study site (behind person on left in B) leaving the upland watershed, slightly dammed by the shutter ridge to the right, and then the offset channel segment traversing the view under the nearer person and turning southwest just outside the view to the right. Trench T2 was dug parallel to the SAF and across the upstream channel mouth approximately where the person on the left crouches, and T3 was dug perpendicular to T2 up onto the shutter ridge. Compare with Figure 5.

Figure 5. Topographic map of the study site with 1-meter contour interval. Channels once connected to the main channel (southeast) have been offset as the three beheaded channels to the northwest. Our trench excavations exposed offset channels in T2, T3, T8, T6', and T7. The T7 channel has subsequently captured the small drainage immediately above it. The cross-section below shows the topographic profile through the beheaded channels (dashed line on map) and the projected channel cross-sections exposed and surveyed in the excavations. Note that the offsets determined by matching the channels defined in the trenches are different than those determined just from the offset geomorphology. Trench locations (closed polygons) are mapped from survey data.

Figure 6a. Lithologic log of northeast wall of Trench 2 (see Figure 5 for location). Several nested channels are cut into the local Paso Robles bedrock unit. The channels are filled with clast-supported gravel which grade outward or are cut into and overlain by colluvial units or channel deposits that have been pedogenically altered. The lowermost channel thalweg (base of unit 210) is the match for the offset thalwegs exposed in T6', T8, and T7. The explanation below indicates the patterns, linetypes, and labels used in all of the logs.

Figure 6b. Lithologic log of the northwest wall of Trench 3 (see Figure 5 for location). This trench exposed three main shear zones that progressively cut up section from southwest to northeast. Grey-green unit 300 is correlative with unit 200 from trench 2 (Figure 6a) and is juxtaposed against highly sheared and deformed tan Paso Robles or older Quaternary units to the southwest. Units 370 and 375 represent the channel fill sequence. The two channel fill packages are separated by a fissure fill unit that probably formed in the 1857 earthquake. See the trench log explanation in Figure 6a.

Figure 6c. Lithologic log of the southwest wall of Trench 6 (see supplemental Figure 1a for the northeast wall and Figure 5 for location). Clast-supported sand and gravel fluvial deposits fill nested channels cut at the base into local Plio-Quaternary bedrock (units 610 and 630). The base of unit 640 is the thalweg offset from the exposures in Trench 2. Importantly, ^{14}C sample T6'-4 dates the colluvium into which the channel was cut, providing a maxium channel age. See the trench log explanation in Figure 6a.

Figure 6d. Lithologic log of the northeast wall of Trench 8 (see supplemental Figure 1b for the southwest wall and Figure 5 for location). Clast-supported sand and gravel fluvial deposits fill nested channels cut at the base into local Plio-Quaternary bedrock (units 810 and 830). The base of unit 840 is the thalweg offset from the exposures in Trench 2. Most of the ^{14}C samples in this study come from the top of unit 860 and provide a minimum channel age. See the trench log explanation in Figure 6a.

Figure 6e. Lithologic log of the northeast wall of Trench 7 (see supplemental Figure 1c for the southwest wall and Figure 5 for location). Because of its older age, the stratigraphic relationships are more obscured than the younger trenches by pedogenesis. Nonetheless, unit 730 has eroded into the local bedrock (a Quaternary fan deposit) and its base represents the thalweg that we correlate with that exposed in Trenches 2, 6' and 8. This channel thalweg is offset about 48.8 m. See the trench log explanation in Figure 6a.

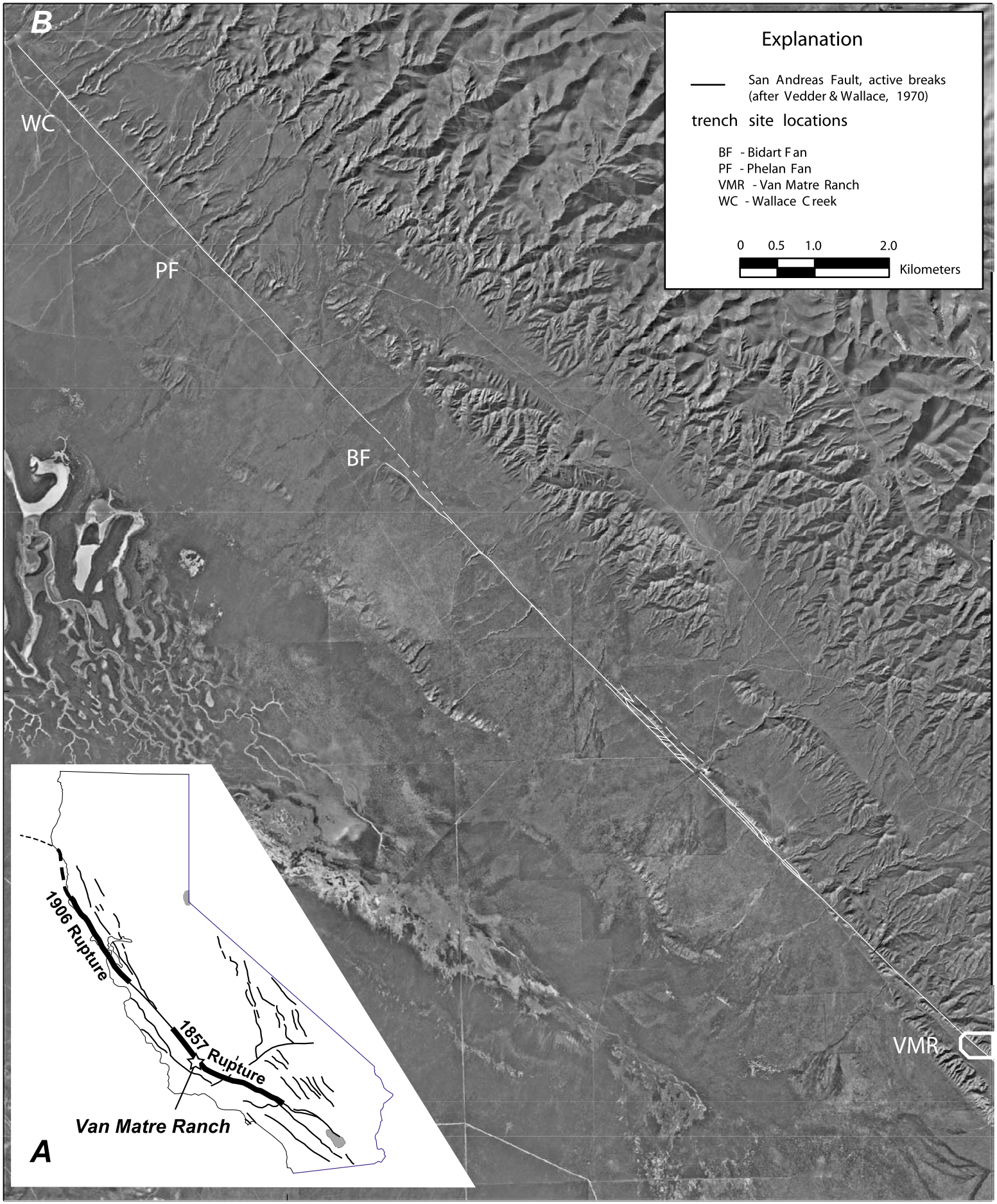

Figure 1. Noriega, et al.

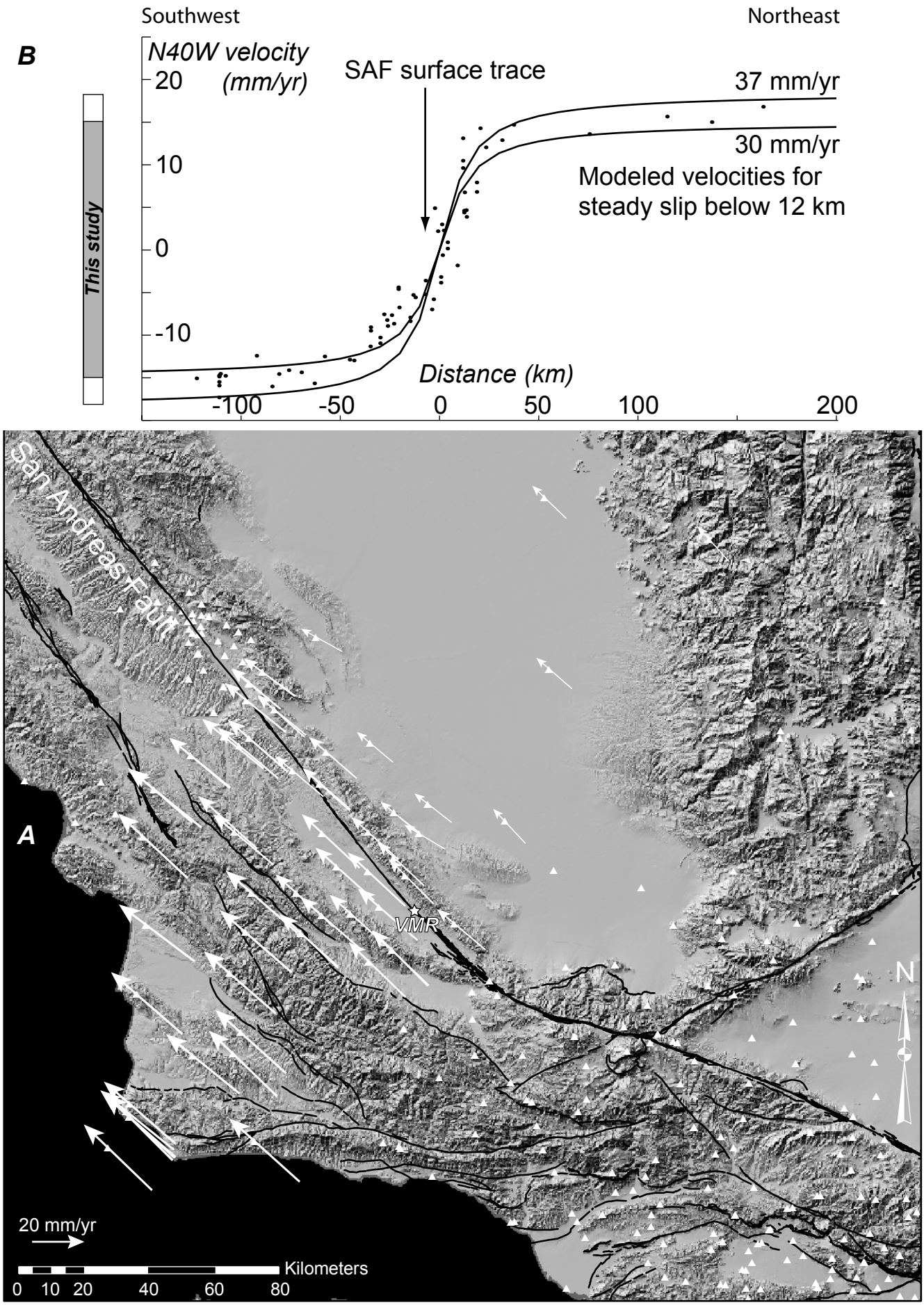

Figure 2. Noriega, et al.

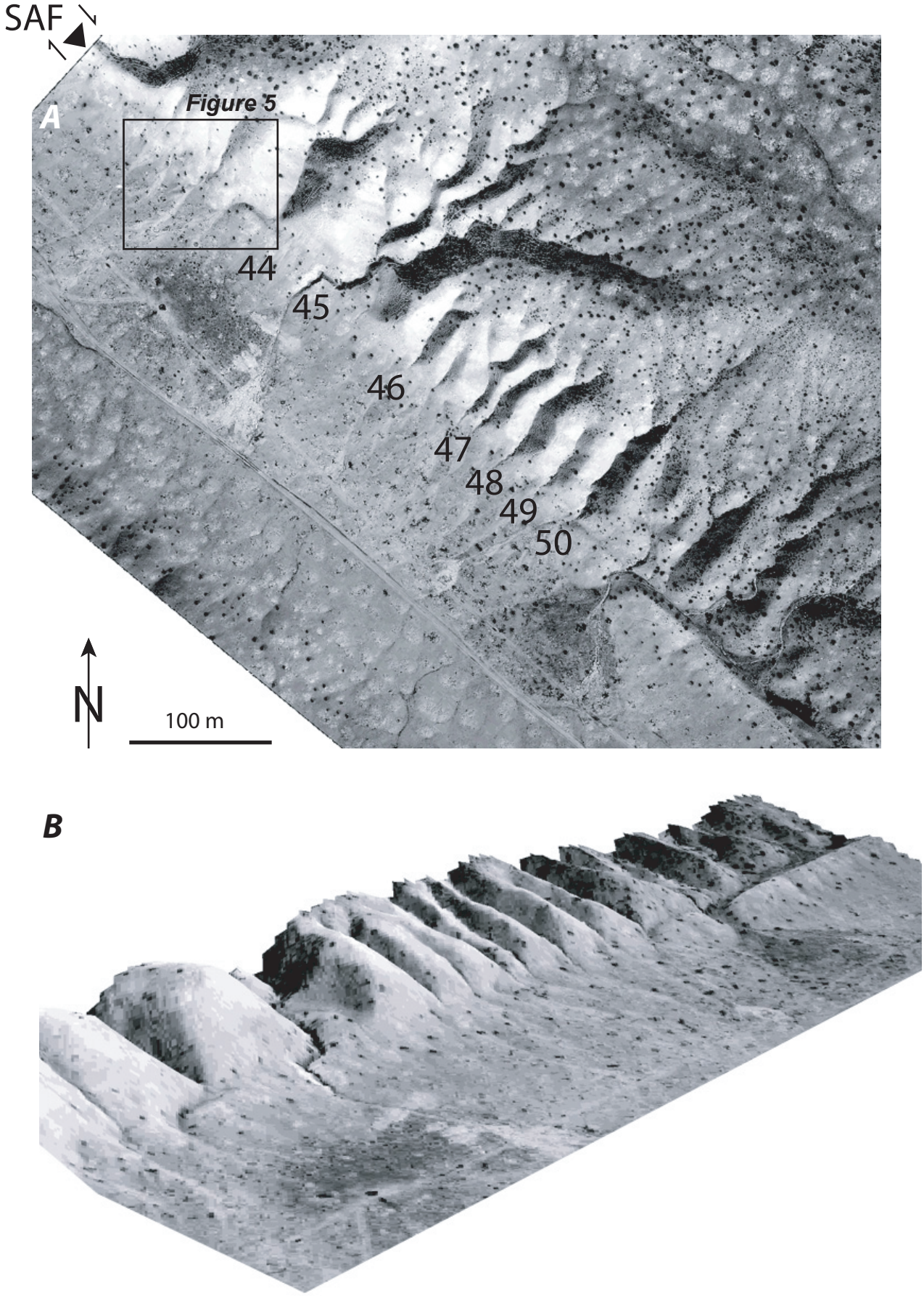

Figure 3. Noriega, et al.

Figure 4. Noriega, et al.

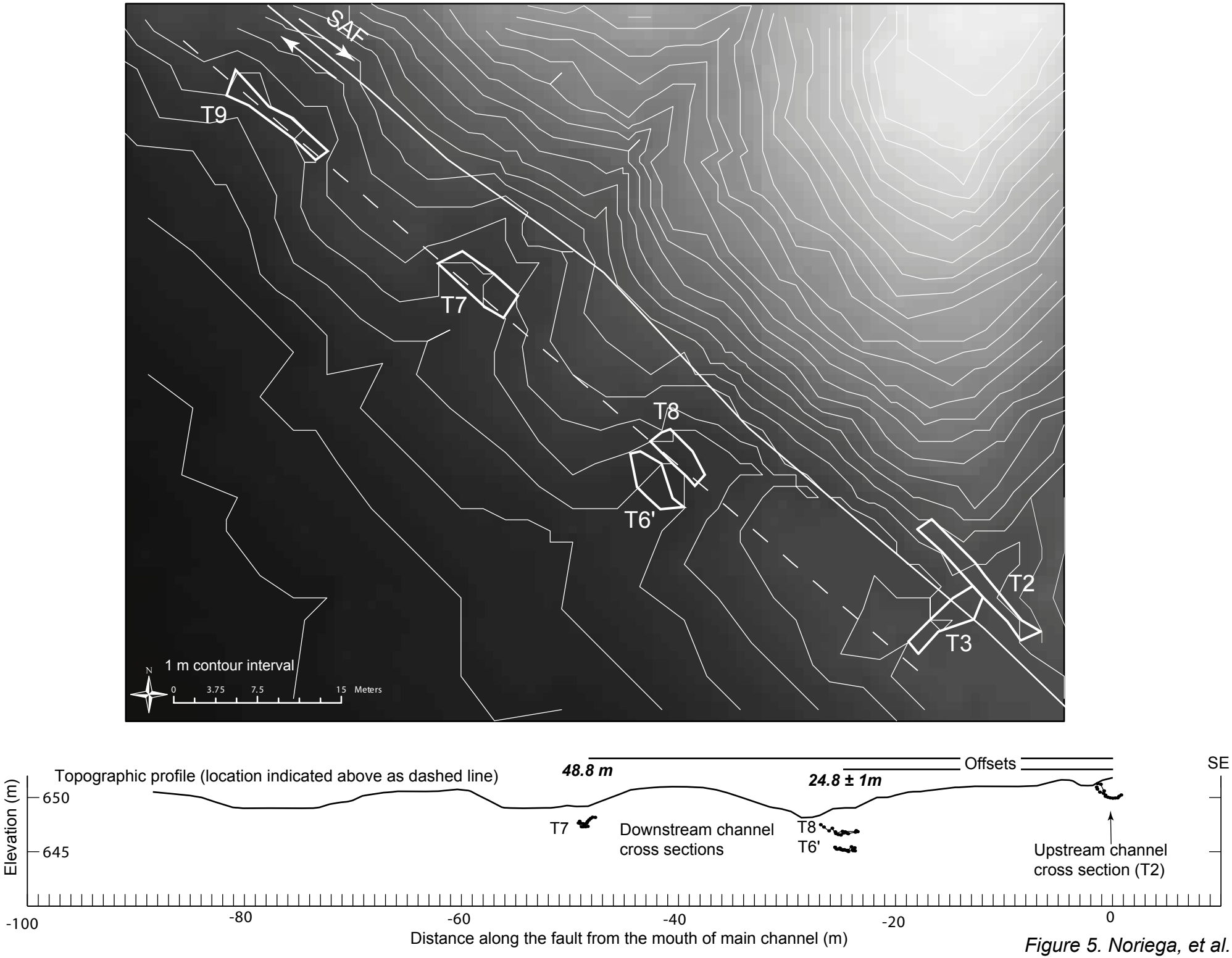

Figure 5. Noriega, et al.

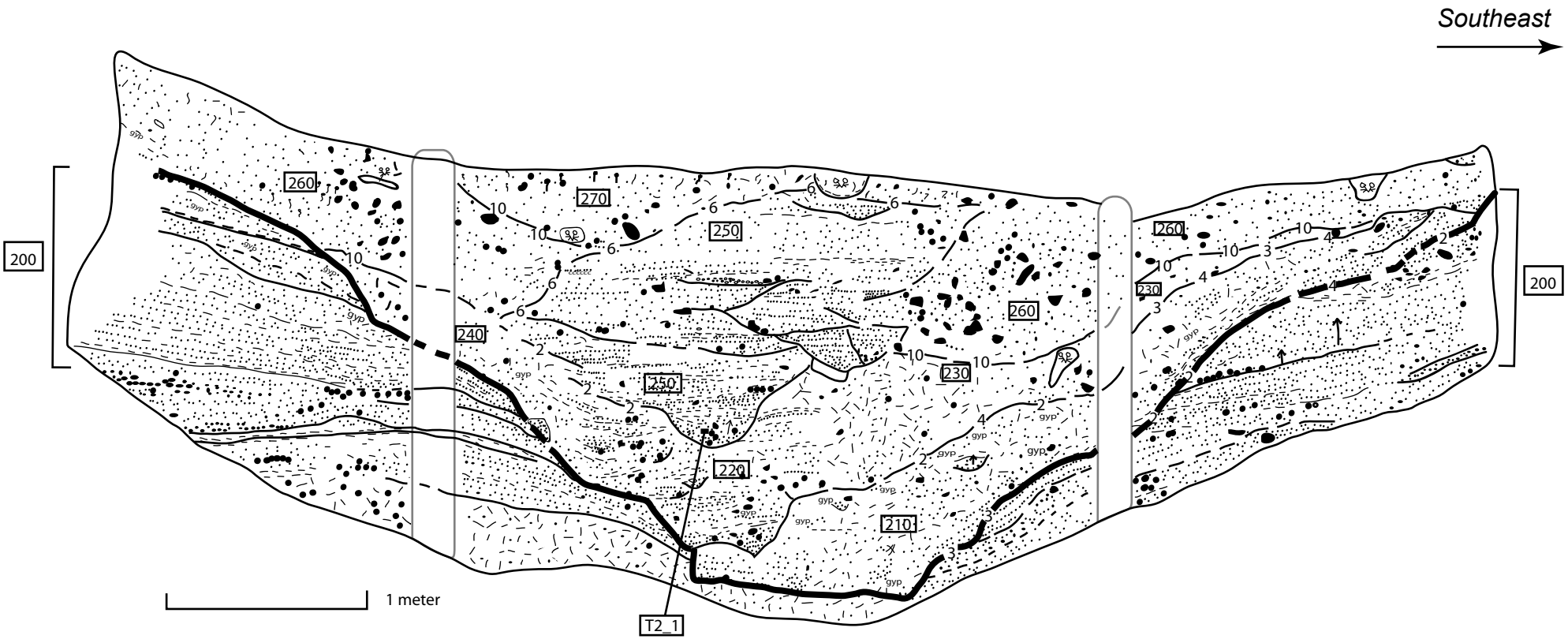

Explanation

Logging symbols

- sharp contact
- approximately located contact
- 8 — gradational contact in cm
- ? ? — location of contact is questionable
- channel contact used to measure offset
- T2_1 — ^{14}C sample location
- 210 — Unit label

Lithologic Symbols

- burrows
- k — carbonate
- gyp — gypsum
- ↑ — fining upward
- carbon sample
- laminated silt
- massive silt
- fine-medium sand
- coarse sand
- cobbles and pebbles
- clay
- colluvium
- cobble or boulder to scale
- granitic boulder to scale

Figure 6a. Noriega, et al.

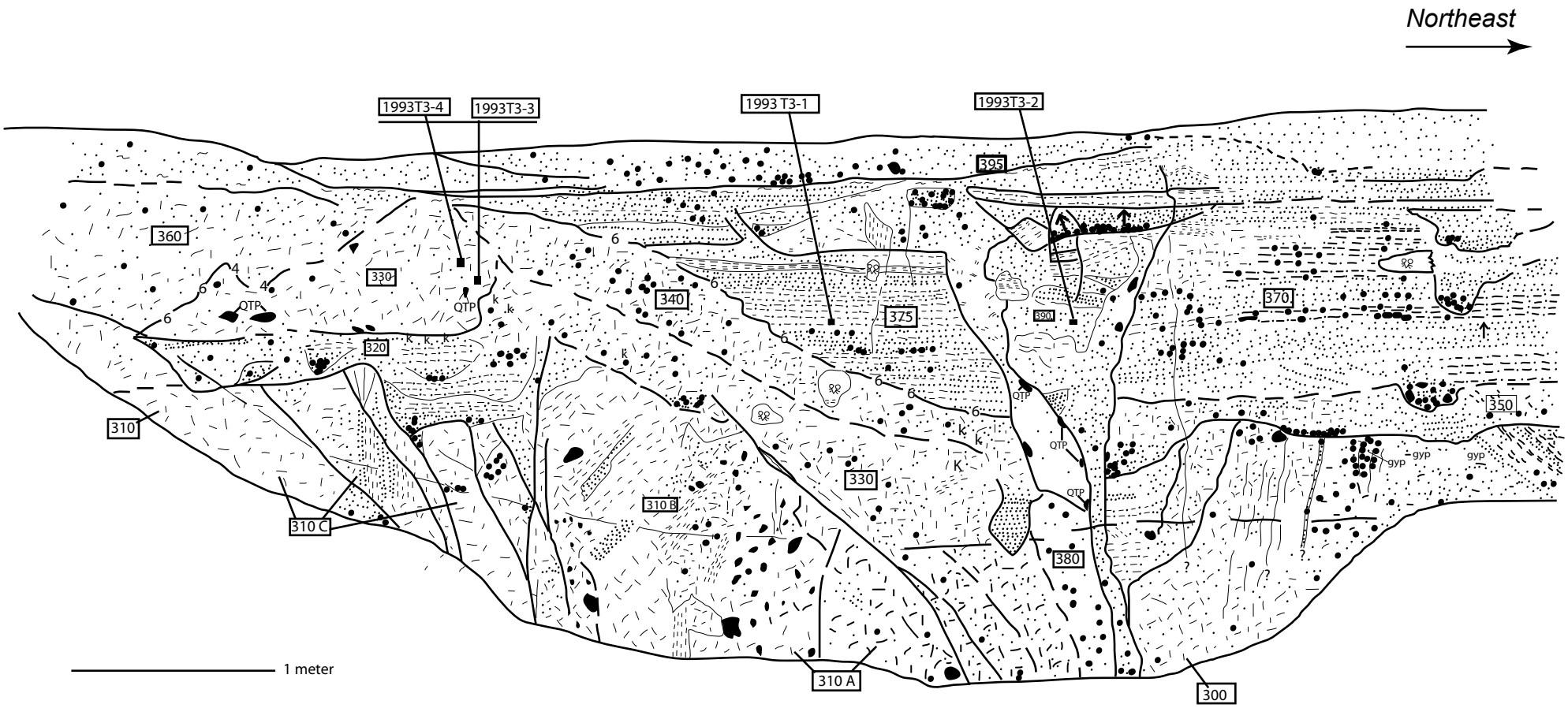

Figure 6b. Noriega, et al.

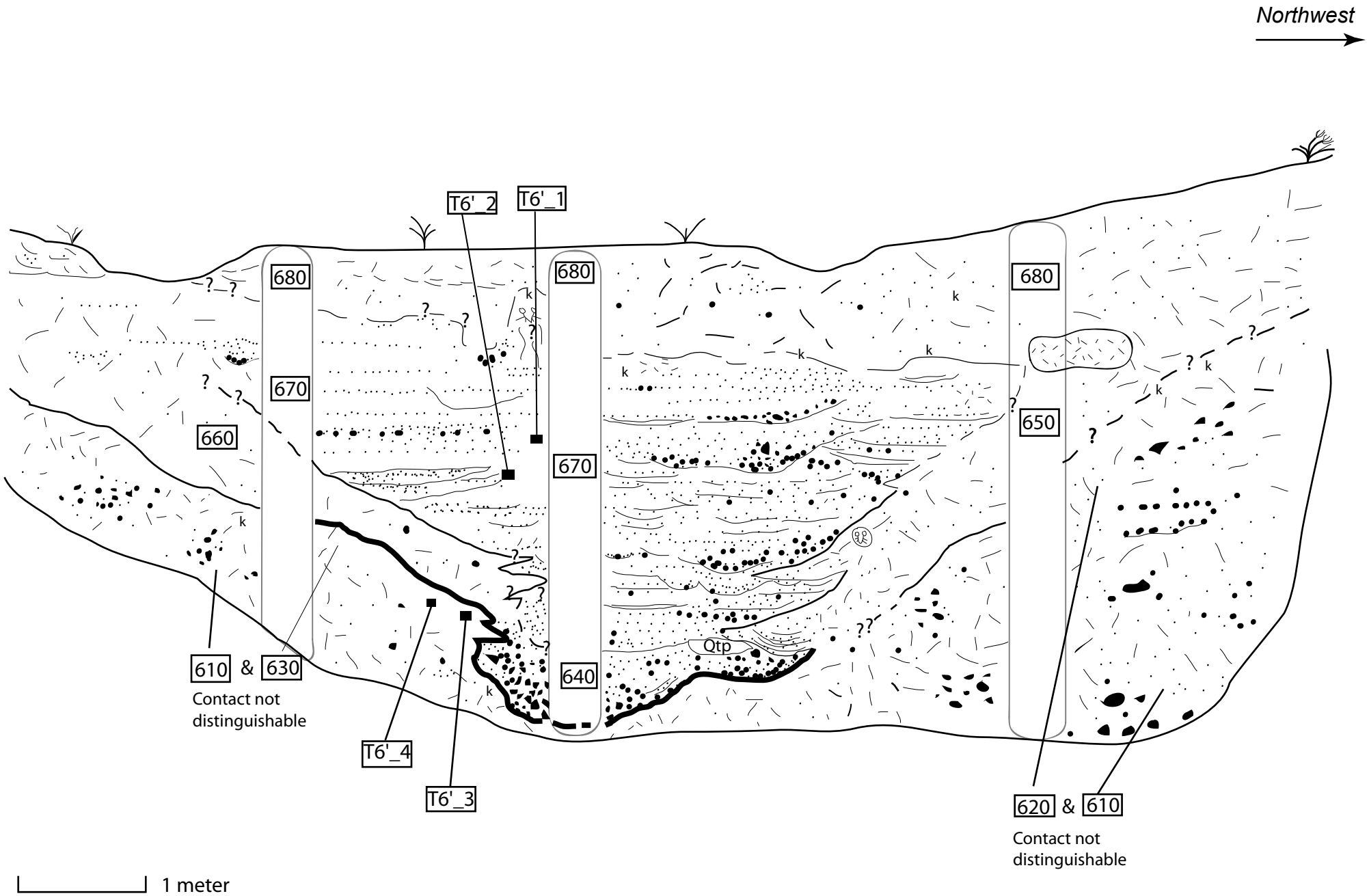

Figure 6c. Noriega, et al.

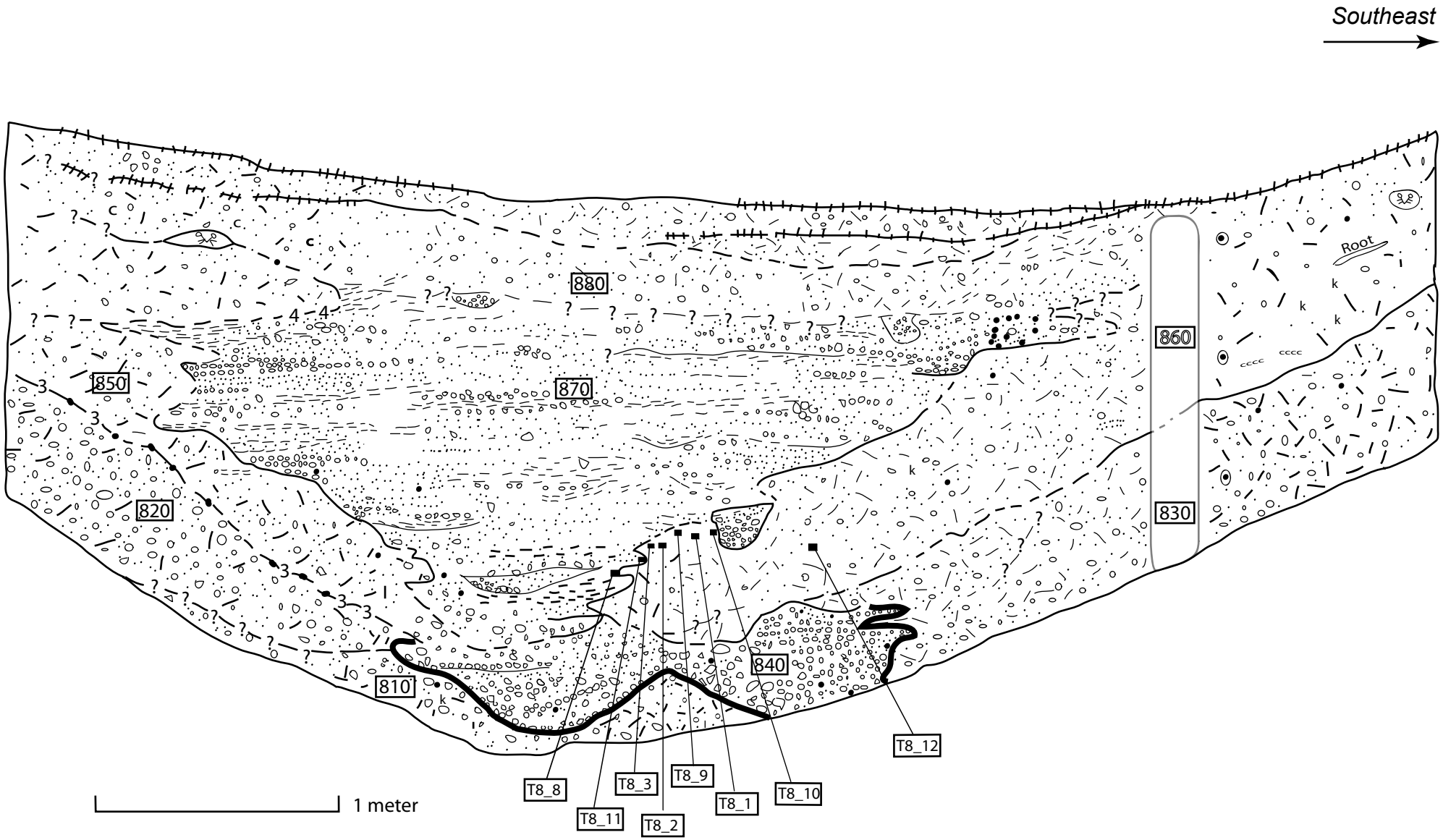

Figure 6d. Noriega, et al.

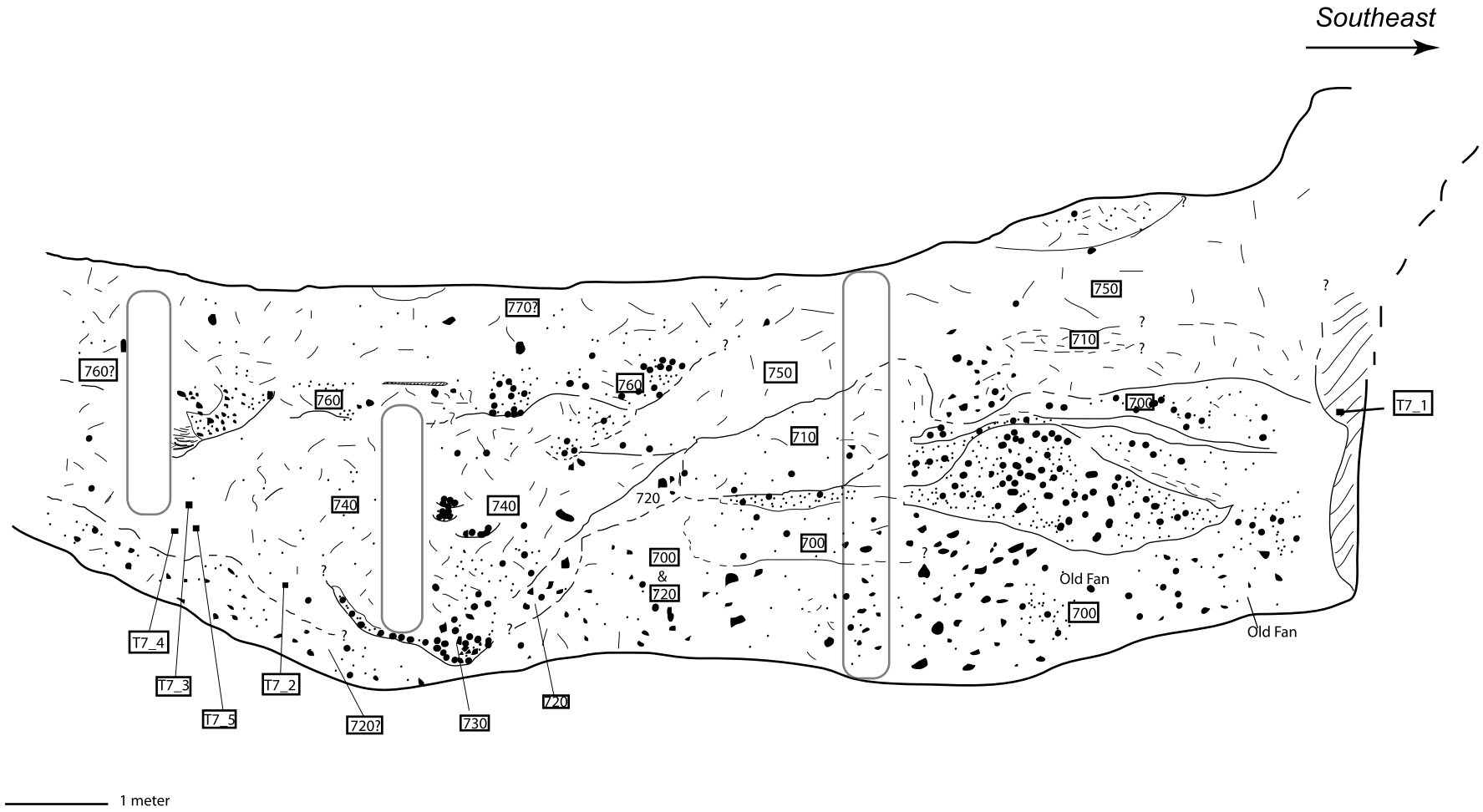

Figure 6e. Noriega, et al.

SUPPLEMENTAL FIGURES

Supplemental Figure 7a. Supplemental lithologic log of the northeast wall of Trench 6 (see Figure 5 for location, Figure 6a for explanation and Figure 6c for corresponding southwest wall).

Supplemental Figure 7b. Supplemental lithologic log of the southwest wall of Trench 8 (see Figure 5 for location, Figure 6a for explanation and Figure 6d for corresponding northeast wall).

Supplemental Figure 7c. Supplemental lithologic log of the southwest wall of Trench 7 (see Figure 5 for location, Figure 6a for explanation and Figure 6e for corresponding northeast wall). The wall was only partially exposed on the southern end. The rest of the trench was covered with fill from 1993 excavations.

Supplemental Figure 7d. Lithologic log for the northeast wall of Trench 9. The lower units are steeply dipping to the northeast and are moderately lithified. Unit 930 may correspond to sediment delivered from the small drainage now captured by the channel mouth cut by T7. None of these units were definitely correlative with the offset channel thalwegs exposed in T2, T6', T8, and T7.

Supplemental Figure 2. Illustration of probability distributions for calendar dates determined from the radiocarbon age for each sample using OxCal v. 3.10 (Bronk Ramsay, 1995, 2001). We summed the cluster of seven non reworked samples from Trench 8 and placed the remaining two samples (T8_11 and T6'_4) in stratigraphic order, thus constraining the maximum age for channel cutting to the approximate minimum age of sample T6'_4 to 1165AD.

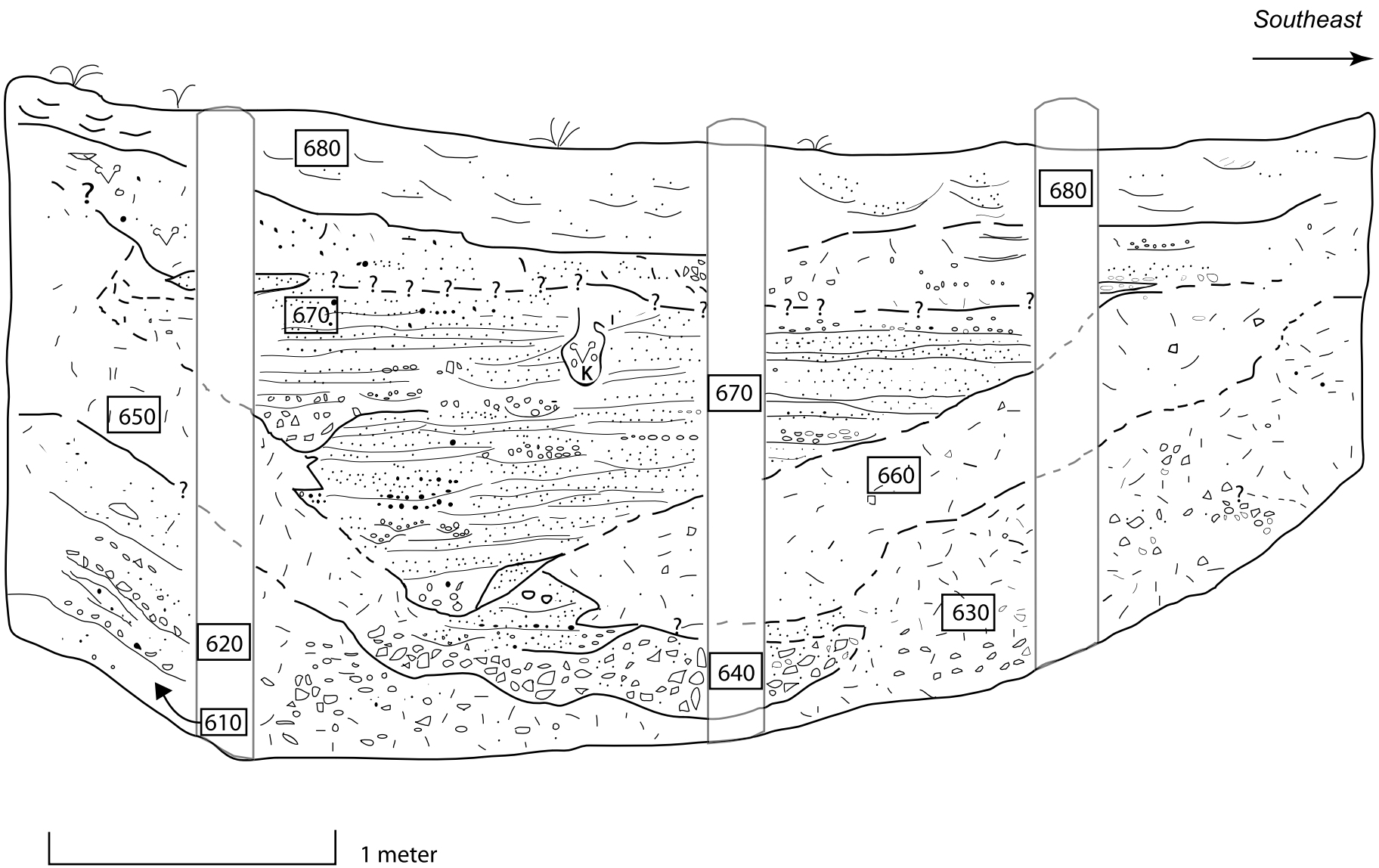

Figure 7a (supplemental). Noriega, et al.

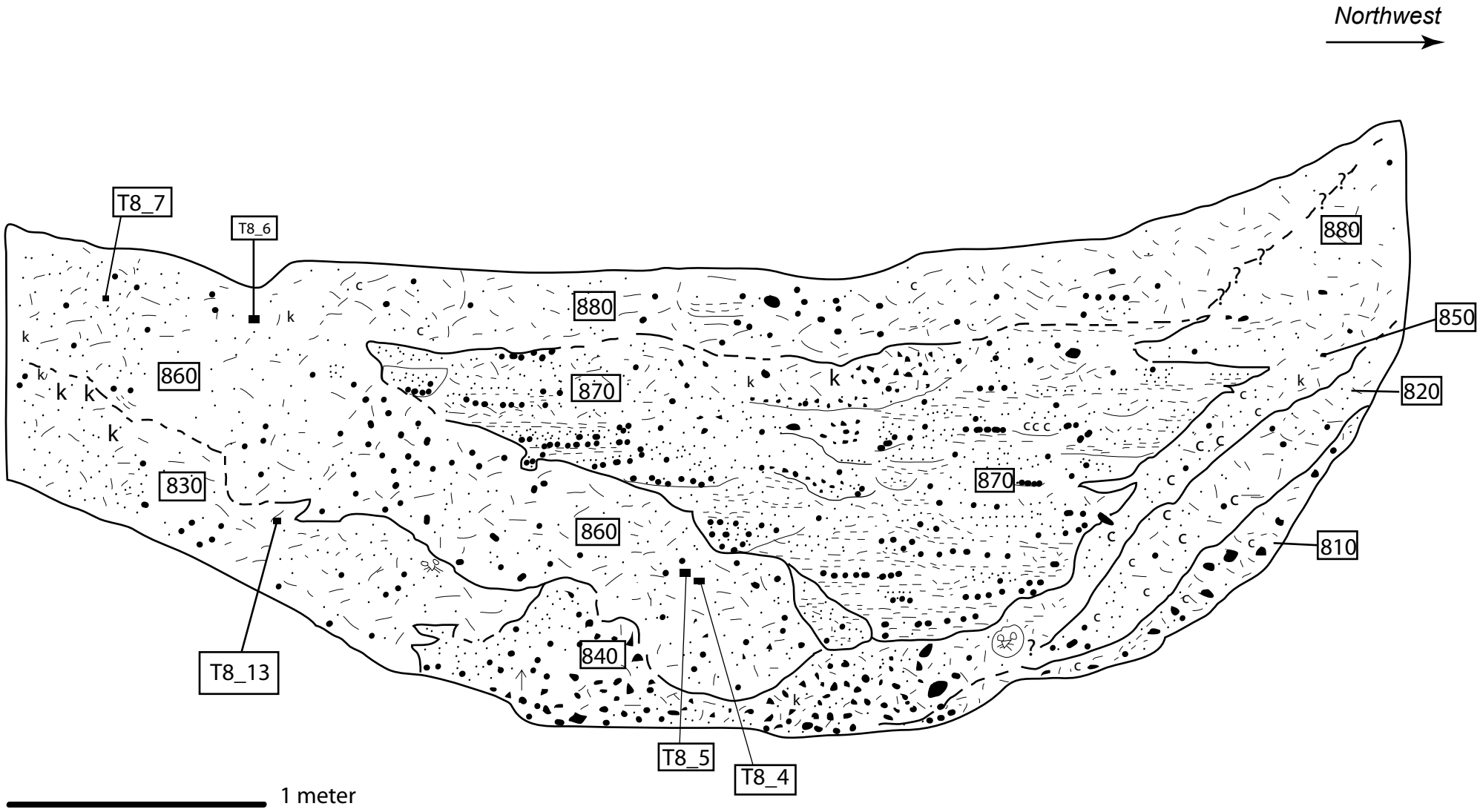

Figure 7b (supplemental). Noriega, et al.

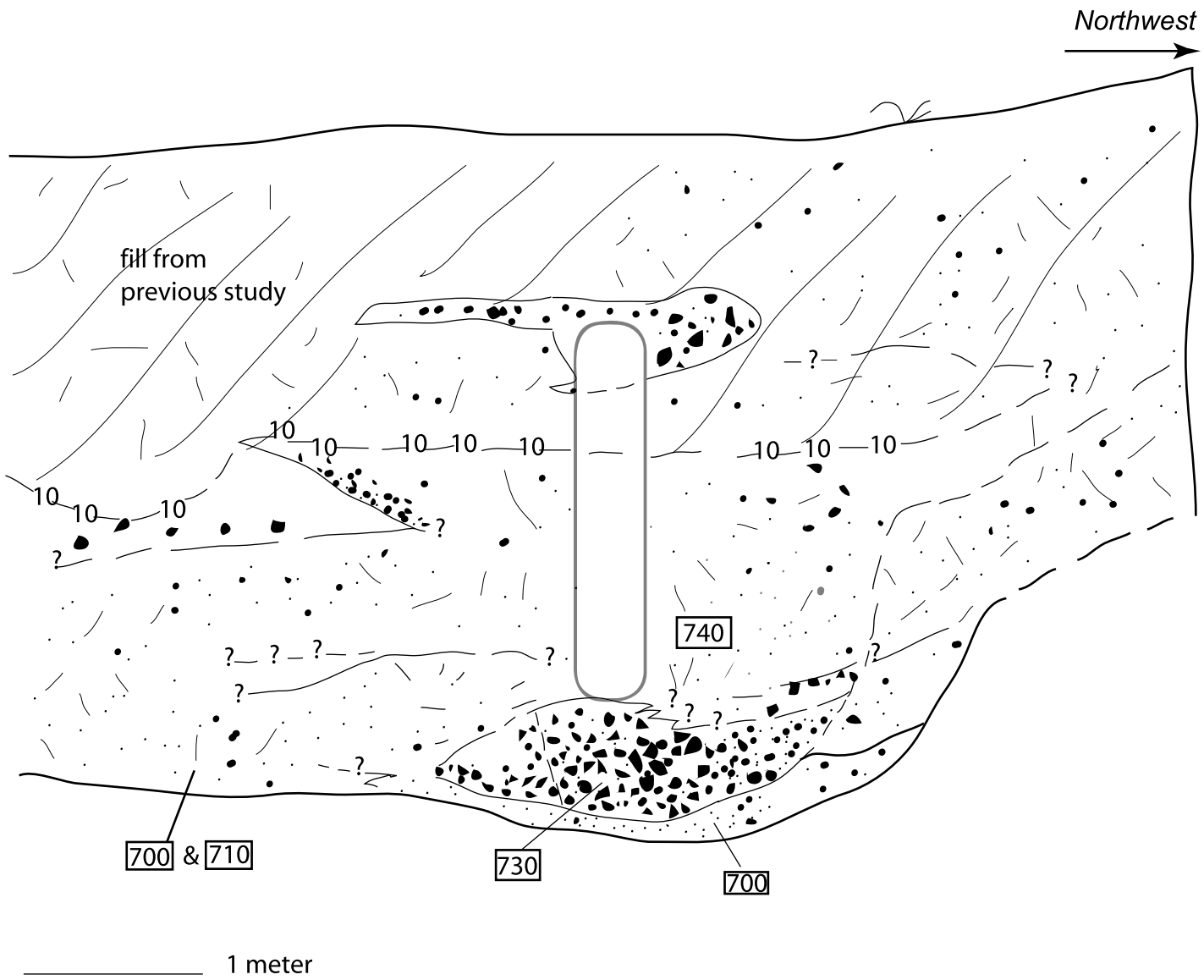

Figure 7c (supplemental). Noriega, et al.

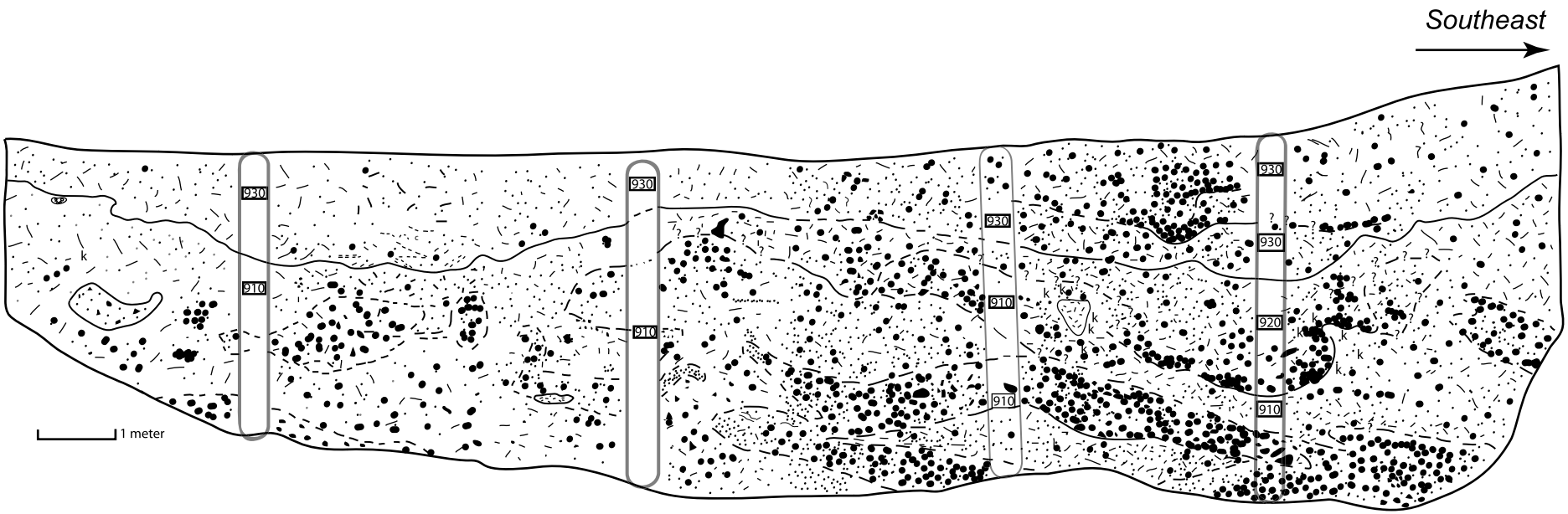

Figure 7d (supplemental). Noriega, et al.

Atmospheric data from Reimer et al (2004);OxCal v3.10 Bronk Ramsey (2005); cub r:5 sd:12 prob usp[chron]

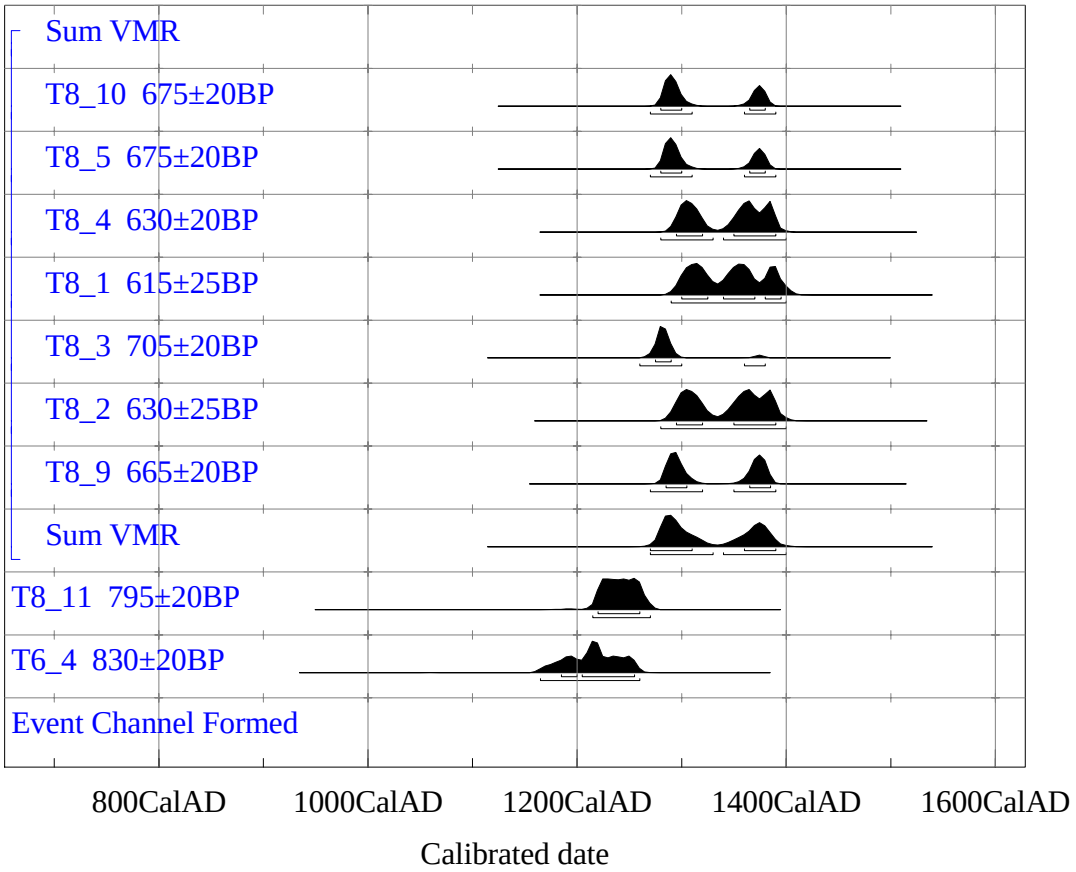

BIBLIOGRAPHY

Argus, D. F. and R. G. Gordon (2001). Present tectonic motion across the Coast Ranges and San Andreas fault system in central California, *Geol. Soc. Am. Bull.* **113**, no. 12, 1580-1592.

Bronk Ramsey, C. (1995) Radiocarbon Calibration and Analysis of Stratigraphy: The OxCal Program *Radiocarbon* **37(2)** 425-430

Bronk Ramsey, C. (2001) Development of the Radiocarbon Program OxCal, *Radiocarbon*, **43** (2A) 355-36

Dibblee, T.W., Jr. (1973). Regional geologic map of San Andreas and related faults in Carrizo Plain, Temblor, Caliente, and La Panza ranges and vicinity, California, Miscellaneous Geologic Investigations Map: Reston, VA, United States, *U. S. Geol. Surv*. p 9.

Grant, L. B., and A. Donnellan (1994). 1855 and 1991 Surveys of the San Andreas fault: Implications for fault mechanics, *Bull. Seism. Soc. Am.*, **84**, no. 2, 241-246.

Grant, L. B., and K. Sieh (1993). Stratigraphic evidence for seven meters of dextral slip on the San Andreas fault during the 1857 earthquake in the Carrizo Plain, *Bull. Seism. Soc. Am.* **83**, 619-635.

Grant, L. B., and K. Sieh (1994). Paleoseismic evidence of clustered earthquakes on the San Andreas fault in the Carrizo Plain, California, *J. Geophys.Res*. **99**, B4, 6819-6841.

Lisowski, M., Savage, J. C. and W. H. Prescott (1991). The velocity field along the San Andreas fault in central and southern California, *J. Geophys. Res*. **96**, 8369-8389.

Liu, J. (2003). Slip behavior of the San Andreas fault through several earthquake cycles. ***Ph.D. dissertation,*** California Institute of Technology, Pasadena, California.

Liu, J., Klinger, Y., Sieh, K., and C. Rubin (2004). Six similar sequential ruptures of the San Andreas fault, Carrizo Plain, California, *Geology* ,**32,** 8, 649-652.

Prentice, C. S. and K. Sieh (1989). A paleoseismic site along the Carrizo segment of the San Andreas fault, central California, *EOS, Trans.*, **70**, 1349.

Sieh, K. E., (1977). Late Holocene displacement along the south-central reach of the San Andreas fault, ***Ph.D. dissertation***, Stanford University, Stanford, CA, p 219.

Sieh, K. E., (1978). Slip long the San Andreas fault associated with the great 1857 earthquake, *Bull. Seism. Soc. Am*. **68**, 1731-1749.

Sieh, K. E., (1979). Geological Studies of the Holocene Behavior of the SAF, CA. *Proceedings of the International Research Conference on Intra-continental Earthquakes*. Ohrid, Yugoslavia.

Sieh, K. E. and R. H. Jahns (1984). Holocene activity of the San Andreas fault at Wallace Creek, California**,** *Geol. Soc. Am. Bull.* **95**, 883-896.

Sims, J. D., (1994). Stream channel offset and abandonment and a 200-year average recurrence interval of earthquakes on the San Andreas fault at Phelan Creeks, Carrizo Plain, California, in *Proceedings of the Workshop on Paleoseismology, U.S. Geol. Surv. Open File Rept. 94-568*, 210 pp.

Sims, J. D., Hamilton, J. C., and Arrowsmith, R., (1993). Geomorphic study of earthquake offsets and subsequent landform response along the San Andreas Fault, Carrizo Plain, California, *EOS Trans.*, **74**, 43, 612.

Stuvier, M., Reimer, P.J. Bard, E., Beck, J. W., Burr, G. S., Hughen, K. A., Kromer, B., McCormac, F. G., V.D. Plight, J., and M. Spurk (1998). INTCAL98 Radiocarbon age calibration 24,000 - 0 BP, Radiocarbon 40, 1041-1083.

Thatcher, W., (1990). Present-day crustal movements and the mechanics of cyclic deformation, in Wallace, R.E., ed., The San Andreas Fault System, California, USGS Prof. Paper 1515, pp.189-205.

Titus, S. J., DeMets, C. and Tikoff, B. (2005). New slip rate estimates for the creeping segment of the San Andreas fault, California, Geology, **33**, 205-208.

Working Group on California Earthquake Probabilities (WGCEP) (1988). Probabilities of large earthquakes occurring in California on the San Andreas Fault, *U.S. Geol. Surv. Open File Rept. 88-398*.

Working Group on California Earthquake Probabilities (WGCEP) (1995). Seismic hazards in southern California: Probable earthquakes, 1994-2024, *Bull. Seism. Soc. Am*. **85**, 379-439.